

**ADAMA SCIENCE AND TECHNOLOGY UNIVERSITY (ASTU)**

**SCHOOL OF APPLIED NATURAL SCIENCE  
APPLIED CHEMISTRY DEPARTMENT**



**SORPTION OF LEAD (II) IONS FROM INDUSTRIAL WASTE WATER  
USING NANOSIZED OXIDES MIXED WITH MAIZE COB SORBENT  
SYSTEM**

**RESEARCH PROJECT**

**Dr. DEREJET.**

**Mr. HIZKEAL TSADE**

**Mr. BUZUAYEHU A.**

**Mss. NEJAT R.**

**October, 2018**

**ASTU, ETHIOPIA**

## ACKNOWLEDGEMENTS

Firstly, we extend our sincere thanks to almighty God for helping us to complete this project research work and for all His help throughout our presence.

Following, extend our sincere and heartfelt thanks to our University (ASTU) Research and Technology Transfer office for giving us research grant and other related office for providing us with all the necessary facilities for the success of this research work within the planned time. Without their encouragement and genuine participation from the very beginning of project work to project output would not have been possible.

We also thank Chemistry Department of **ASTU** due to their help for effective realization of this work. Additionally, we thank Chemistry Department of **AAU** for their cooperation in the running of the FTIR and XRD characterization effectively.

We also thank Mr. Guta Amanu and Mr. Tolosa Duguma academic and research assistance of Chemistry program in the ASTU their voluntary assistance during hybrid adsorbent synthesis, solution preparation and any other activities in the laboratory by sacrificing their extra time.

Finally, we express our heartfelt thanks to our families for their continuous moral support for the success of the study.

## **ABBREVIATIONS AND ACRONYMS**

<b>AG</b>	Analytical Grade
<b>DDW</b>	Double Distilled Water
<b>FAAS</b>	Flame Atomic Absorption Spectrometry
<b>FTIR</b>	Fourier Transform Infrared
<b>NP</b>	Nano Particle mixed oxide
<b>NP-MC</b>	Nano Particle mixed oxide with Maize Cob
<b>MC</b>	Maize Cob
<b>WHO</b>	World Health Organization
<b>SEM</b>	Scanning Electron Microscopy
<b>XRD</b>	X-Ray Diffraction
<b>EDX</b>	Energy-Dispersive X-ray
<b>FWHM</b>	Half Maximum of the major diffraction band
<b>D<sub>s</sub></b>	Primary Crystallite
<b>ICCEA</b>	International Conference on Chemical Engineering and its Applications

## TABLE OF CONTENTS

<b>ACKNOWLEDGEMENTS .....</b>	<b>ii</b>
<b>ABBREVIATIONS AND ACRONYMS .....</b>	<b>iii</b>
<b>LIST OF TABLES.....</b>	<b>vii</b>
<b>LIST OF APPENDIX FIGURES.....</b>	<b>ix</b>
<b>LIST OF APPENDIX TABLES.....</b>	<b>x</b>
<b>Abstract.....</b>	<b>xi</b>
<b>1. INTRODUCTION.....</b>	<b>1</b>
<b>1.1. General Objective .....</b>	<b>3</b>
<b>1.2. Specific Objectives .....</b>	<b>3</b>
<b>2. LITERATURE REVIEW .....</b>	<b>4</b>
<b>2.1. Sources of Water Pollution .....</b>	<b>4</b>
2.1.1. Chromium .....	5
2.1.2. Lead .....	5
2.1.3. Cadmium.....	6
<b>2.2. Current Heavy Metal Ions Removal Technologies .....</b>	<b>7</b>
<b>2.3. Applications of Nanoscale materials in Heavy Metal ions Removal .....</b>	<b>8</b>
2.3.1. Multi Component Nano-Sorbents .....	8
<b>2.4. Adsorption .....</b>	<b>10</b>
2.4.1. Fundamentals of Adsorption.....	10
2.4.2. Langmuir adsorption isotherm.....	12
2.4.3. Freundlich adsorption isotherm .....	13
<b>2.5. Kinetics of Adsorption.....</b>	<b>13</b>
<b>2.6. Thermodynamic of Adsorption .....</b>	<b>14</b>
<b>2.7. Regeneration.....</b>	<b>15</b>
<b>3. MATERIAL AND METHODS.....</b>	<b>16</b>
<b>3.1. Experimental Site .....</b>	<b>16</b>
3.1.1 Apparatus and Instruments .....	16
3.1.2. Chemicals and Reagents .....	16

<b>3.2. Experimental Procedure.....</b>	<b>16</b>
3.2.1. Collection and Preparation of Maize Cob (MC).....	16
3.2.2. Synthesis of Nano-Sized Mixed Oxide.....	17
3.2.3. Synthesis of nano-sized mixed oxide/natural sorbent .....	17
<b>3.3. Characterization of the as-synthesized powder (solid-phase characterization).....</b>	<b>17</b>
<b>3.4. Wastewater Sample Collection and Digestion.....</b>	<b>18</b>
3.4.1. Stock solutions of metal ions .....	18
<b>3.5. Adsorption studies .....</b>	<b>19</b>
3.6.1. Adsorption isotherms .....	19
3.6.2. Kinetics of adsorption.....	20
3.6.3 Thermodynamics of adsorption .....	20
3.6.4. Desorption of Metal ion.....	20
<b>4. RESULTS AND DISCUSSION.....</b>	<b>21</b>
<b>4.1. Synthesis and Characterization .....</b>	<b>21</b>
4.1.1. X-ray diffraction (XRD .....	21
4.1.2. Scanning Electron Microscope (SEM) and EDX Analysis .....	22
4.1.3. Infrared Spectroscopic Studies .....	23
<b>4.2. Adsorption Mechanism .....</b>	<b>24</b>
4.2.1. Effect of pH .....	25
4.2.2. Effect of adsorbent dose .....	25
4.2.3. Effect of contact time.....	26
4.2.4. Effect of speed of agitation.....	27
4.2.5. Effect of initial Metal ions concentration .....	28
4.2.6. Kinetics of adsorption.....	29
4.2.7. Adsorption isotherm .....	31
4.2.8. Thermodynamics of adsorption .....	32
4.2.9. Desorption of lead.....	33
4.2.10. Comparison of the method with others.....	34
<b>5. CONCLUSION AND RCOMMENDATIONS.....</b>	<b>35</b>
<b>5.1. Conclusion .....</b>	<b>35</b>
<b>5.2. Recommendations .....</b>	<b>35</b>

**6. REFERENCES..... 37**  
**7. APPENDIX ..... 41**

## LIST OF TABLES

Table 1: Type of isotherm for various RL. ....	13
Table 2: Langmuir and Freundlich isotherm constants for Pb (II) ions adsorption by Fe-Al-MC sorbent.....	31
Table 3: The values of parameters and correlation coefficients of kinetic models.....	32
Table.4 Thermodynamic parameters for Pb(II) ions adsorption by Fe-Al-MC sorbent. ....	33
Table 5. Comparative data for different adsorbents adsorb different metals.....	34

## LIST OF FIGURES

Fig. 1: Small part of possible lignin structure .....	2
Figure 2. XRD pattern of as synthesized powders.....	21
Figure 3.SEM micrographs with EDX analyses of NP-MC sorbent system. ....	22
Figure 4. FT-IR Spectrum of nano sized oxide mixed with MC sorbent. ....	23
Figure 5. The schematic representation of $Pb^{2+}$ ions adsorbed onto the Fe-Al-MC adsorbent.....	24
Figure 6.Effect of pH on the removal of lead ions. ....	25
Figure 7. Effect of adsorbent dose on the removal of Pb (II) ions .....	26
Figure 8. Effect of contact time optimization on the removal of Pb(II) ions .....	27
Figure 9. Effect of speed of agitation on the removal of Pb (II) ions .....	28
Figure 10. Effect of initial concentration of Pb (II) ions .....	29
Figure 11.Kinetics of Adsorption on the removal of Pb(II) ions . ....	30
Figure 12. Langmuir (a) and Freundlich (b) adsorption isotherm of $Pb^{2+}$ ions by nanosized mixed oxide with MC sorbent at pH = 6.....	31
Figure 13.Plot of $\ln K_c$ vs $T^{-1}$ for Pb(II) ions adsorption .....	33
Figure 14. Effect of pH on desorption of Pb(II) ions .....	34

## LIST OF APPENDIX FIGURES

Appendix figure1 .Calibration curve for Fe (b), Al (a) (AAS reading). .....	42
Appendix figure 2. Calibration curve of lead for pH (a) and dose (b) optimization. ....	42
Appendix figure 3. Calibration curve of lead for contact time (a) and agitation speed (b) optimization. ....	42
Appendix figure 4. Calibration curve of lead (a) initial lead concentration optimization and kinetics adsorption study (b).....	43
Appendix figure 5. Calibration curve of lead for selectivity (a) and thermodynamic study (b)...	43
Appendix figure 6. Calibration curve of lead for desorption.....	43

## LIST OF APPENDIX TABLES

Appendix Table1. Designation of percentage composition of the as-synthesized powders .....	44
calcined at 600°C and 400°C A and B respectively. ....	44
Appendix Table 2. Effect of pH on adsorption capacity of the nanoparticle mixed with maize cob adsorbents.....	44
Appendix Table 3. Effect of adsorbent dose on adsorption capacity of the nanoparticle mixed with maize cob adsorbents .....	44
Appendix Table 4. Effect of contact time on adsorption capacity of the nanoparticle mixed with maize cob adsorbents .....	44
Appendix Table 5. Effect of agitation speed on adsorption capacity of the nanoparticle mixed with maize cob adsorbents .....	45
Appendix Table 6. Effect of initial Pb (II) ion concentration on adsorption capacity of the nanoparticle mixed with maize cob adsorbents .....	45
Appendix Table 7. Effect of kinetic study on adsorption capacity of the nanoparticle mixed with maize cob adsorbents .....	45
Appendix Table 8. Results for Pb (II) adsorption isotherm on adsorption capacity of the nanoparticle mixed with maize cob adsorbents .....	46
Appendix Table 9. RL values for lead adsorption at different concentration. ....	46

## **Sorption of Pb(II) ions from Industrial Waste Water using Nanosized Oxides Mixed with Maize Cob (MC) Sorbent System**

### **Abstract**

The present work involves the synthesis, characterization and sorption behavior of nano sized Fe-Al mixed oxide with natural maize cob (MC) sorbent for the removal of Pb (II) ions from industrial waste water. The Fe-Al-MC nanocomposite sorbent was synthesized by impregnation method. X-ray diffraction (XRD), Energy-dispersive X-ray (EDX) and scanning electron microscopy (SEM) techniques were applied to study the surface structure, compositions and morphology of the materials. Fourier transform infrared technique was used to analyze the effect of surface properties on the adsorption behavior of Pb (II) ions. The optimum effects of the parameters on the adsorption of Pb (II) ions were determined to be, pH = 6, dose = 2 g, contact time = 7h and agitation speed = 150 rpm and initial Pb (II) ions 10 ppm. Experimentally, the adsorbed amounts of lead ion tend to decrease with increase in pH. Both Langmuir ( $R^2 = 0.997$ ) and Freundlich ( $R^2 = 0.995$ ) isotherm models fit the equilibrium data well on the nanoparticle mixed oxides with MC adsorbent. Kinetic data correlated well with the pseudo second order kinetic model. Thermodynamic studies resulted in negative  $\Delta G$  value indicating the spontaneity of the sorption process. The Fe-Al-MC nanocomposite sorbent showed a sorption capacity of  $40.00 \text{ mg g}^{-1}$  at pH 6. The sorption efficiency of the Fe-Al-MC sorbent was found to be greater than 98.0%. Therefore, this adsorbent with large sorption capacity and efficiency is a promising adsorbent for the removal of Pb (II) ions from the wastewater.

**Keywords:** Nano-sized Fe-Al Oxides, Maize Cob, Impregnation, Adsorbent, Lead ions

# 1. INTRODUCTION

Currently, a serious environmental and public concern all over the world was water pollution by heavy metals due to the increased industrialization and urbanization processes. Some of the toxic metals (e.g., lead, cadmium, chromium, etc.) even at trace levels are believed to pose adverse effects on the human health (Zhao G., et al., 2011, Hardiljeet K., et al., 2013). Wastewater from industries such as, chemical, battery, metallurgical, leather tanning, and mining, contain many toxic heavy metal ions (Chen C. and Wang X. 2006). These wastewaters with toxic heavy metal ions (e.g., lead, cadmium, chromium etc.) are discharged into natural water directly, not only threat the aquatic organisms, but may be enriched by precipitation, adsorption, and harm human health through the food chain (Gupta et al., 2013, Kardam et al., 2014). This forms the basis for the increasing researches with a view to remedying their levels in the environment; and also the growing concern by governmental agencies for the regulation of the discharge of these metals into the environment.

Several heavy metal remediation methods are available to minimize the pollutant levels in water and wastewater, including chemical oxidation and reduction, membrane separation, liquid extraction, ion exchange, electrolytic treatment, electroprecipitation, coagulation, flotation, evaporation, hydroxide and sulfide precipitation, crystallization, ultrafiltration, and electro dialysis and they differ in their effectiveness and cost (Fu, F. and Wang, Q. 2011, Gupta, V.K. and Ali, I. 2013). Among these, adsorption using activated carbon has been considered as one of the best choice methods for water and wastewater remediation due to its high removal efficiency without the production of harmful by-products (Bhatnagar et al., 2013, S. Hokkanen et al., 2016).

Different materials, such as activated carbons (Kobya M., et al., 2005), clay minerals (Oubagaranadin J U K and Murthy Z V P 2009) chelating materials (Gao C et al., 2008) and chitosan/natural zeolites (Sun S., Wang L., Wang A. 2006) have been investigated to adsorb metal ions from aqueous solutions. In the 1940's, activated carbon was introduced for the first time as the water industry's main standard adsorbent for the reclamation of municipal and industrial wastewater to a potable water quality (Kurniawan et al., 2006). It has been found as a versatile adsorbent due to its high capacity towards various pollutants because of high surface

area and well developed porous structure. Production of activated carbon is relatively complicated and involves carbonization and activation stages. In spite of this, activated carbon could not be used as adsorbent for large scale water treatment in poor or developing countries due to its high cost of production. In addition to this, in spite of their high up take capacities the large-scale use of nano sized oxides alone is quite limited because of the difficulties raised in the dispersion of powdered adsorbents, several aggregation formed due to loss of solubility and the need of higher costs of regeneration. Therefore, nanosized oxides mixed with natural adsorbents have proven to be an efficient and inexpensive option for the adsorption of heavy metals from wastewater (Rafika S et al., 2009).

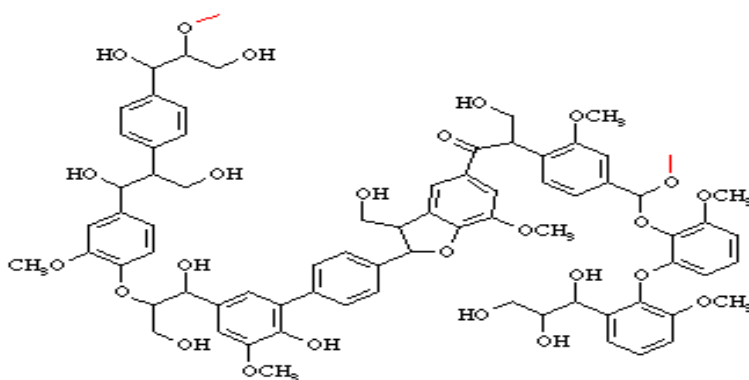


Fig. 1: Small part of possible lignin structure

MC is mainly composed of lignocellulose materials (figure 1) having relatively large surface areas that can provide intrinsic adsorptive sites to many substrates and inherently adsorb waste chemicals such as organic pollutants, inorganic pollutants and atmospheric pollutants in water due to columbic interaction and physical adsorption.

Nano sized metal oxides are used as the novel adsorbent to remove heavy metal ions from wastewater due to their higher efficiency (higher surface areas) and faster kinetics (intraparticle diffusion). An efficient sorbent with both high adsorbing capacity and fast rate adsorption should have the following two main characteristics: functional groups and large surface area (Huang M.R, Huang S.J, Li X.G. 2011). Recently, the development of hybrid sorbents will fulfill these two main characteristics for removal of heavy metals from water (Pan B., et al., 2009, Zhao X., et al., 2011).

As per the knowledge of the author, since no research work has been conducted on the sorption characteristics of nano-sized mixed oxides with natural sorbents for the removal of heavy metals and its easy synthesis, environmentally friendly, easy regeneration after adsorption and having high uptake capacity was aimed to synthesize Fe-Al-MC sorbent, characterize Fe-Al-MC sorbent and to study its lead sorption behavior. This novel sorbent is believed to exhibit superior adsorption efficiency as it possesses high surface areas and with enhanced functional groups on its surface due to the composite nanoadsorbent properties. The sorption kinetics, sorption isotherms, regeneration, influence of solution pH and coexisting ions on Pb (II) ions uptake were investigated. Finally, the outcome of this study may possibly serve as the basis for the remediation of wastewater on an industrial scale.

### **1.1. General Objective**

- To synthesize, characterize and study sorption behavior of nano sized oxides mixed with natural sorbent system for removal of Pb (II) from industrial waste water.

### **1.2. Specific Objectives**

- ❖ To synthesize nano sized oxides mixed with natural sorbent system for removal of toxic heavy metals from industrial waste water.
- ❖ To characterize the as-synthesized material by using modern spectroscopic techniques such as FT-IR, XRD, SEM and EDX.
- ❖ To investigate the Pb (II) ions sorption behavior of the as-synthesized Adsorbent
- ❖ To regenerate the adsorbent from the metal loaded powder.

## 2. LITERATURE REVIEW

### 2.1. Sources of Water Pollution

Water pollution can be defined as any physical, biological, or chemical changes in water quality that adversely affects living organisms or makes water unsuitable for desired uses. The main sources of pollution that enters urban surface water bodies are either point or non-point sources including industries, municipal solid wastes or oily wastes from garages and fuel stations (Keng et al., 2013). There are over 2,000 registered industries found in our capital city of Ethiopia, Addis Ababa (65 % of all industries in the country) most of them located along the river banks. According to the Addis Ababa Environmental Pollution Authority (2007 unpublished), 90% of all industries lack facilities for some degree of onsite treatment plant, and subsequently discharge any effluents into adjacent streams.

The most serious water pollutants discharged from the different sources in the worldwide are both bacterial and viral, nitrates from fertilizer use, heavy metals from soil and urban runoff, mineral oil discharges from illegal dumping, chlorinated solvent discharges from poorly managed waste disposal sites, acid rain, and a cocktail of poisons from working industrial and mineral sites (Kardam et al., 2014, Hokkanen et al. 2016). Many of these pollutants have great tendency for bioaccumulation in the food chain as they are not biodegradable in nature (Keng et al., 2013). Among these, the contamination of water with heavy metals is a serious cause of environmental and human health problems (O'Connell *et al.* 2008). This is due to, unlike organic pollutants heavy metals are non-biodegradable and can be accumulated in living tissues, causing various diseases and disorders, since they can be toxic and/or carcinogenic (Wang JL. and Chen, C., 2009, Fu and Wang 2011).

The term “heavy metal” is entirely applied to a group of metals (and metal-like elements) with density greater than 5 g/cm<sup>3</sup>, atomic number above 20 and is toxic or poisonous at low concentrations (Raut, N. et al., 2012). Three kinds of heavy metals were of concern, including toxic metals (such as Hg, Cr, Pb, Zn, Cu, Ni, Cd, As, Co, Sn, etc.), precious metals (such as Pd, Pt, Ag, Au, Ru etc.) and radionuclides such as U, Th, Ra, Am, etc. (Raut, N. et al., 2012). The most common toxic heavy metals in wastewater include arsenic, lead, mercury, cadmium,

chromium, copper, nickel, silver, and zinc. Heavy metals are natural components from the earth's crust. They cannot be destroyed or degraded. However, most of these heavy metals become toxic at high concentrations due to their ability to accumulate in living tissues. Removal of heavy metals from industrial wastewater is of primary importance. Cadmium, zinc, copper, nickel, lead, mercury and chromium are often detected in industrial wastewaters.

### **2.1.1. Chromium**

There were two stable oxidation states of chromium found in the environment, Cr (III) and Cr (VI) which have contrasting toxicities, mobility and bioavailability. Oxidation state  $\text{Cr}^{6+}$  chromium compounds were considered as powerful oxidants. Hexavalent chromium Cr(VI) compounds were used as pigments for Photography, and in pyrotechnics, dyes, paints, inks, and plastics. They could also be used for stainless steel production, textile dyes, wood preservation, leather tanning, and as anti-corrosion coatings. While Cr (III) is relatively innocuous and immobile, Cr (VI) moves readily through soils and aquatic environments and is a strong oxidizing agent capable of being absorbed through the skin. For normal carbohydrate and lipid metabolism, an essential element required was trivalent chromium, Cr (III).

US Environmental Protection Agency (EPA) indicates that the allowed contamination level for chromium ion in potable water is 0.1 mg/L, while the concentration of the discharge to inland surface water is 0.5 mg/L (USEPA, 1983). Adsorption is the sufficient technique for Cr (VI) removal from industrial wastewater (Badruddoza AZMd et al., 2013). The guideline prescribed by the World Health Organization (WHO) for Cr (VI) in drinking water is 16 mg/L (WHO, 2008). The effluent from industries containing Cr (VI) is considered by the International Agency for Research on Cancer (IARC) (1982) as a powerful carcinogenic agent that modifies the DNA transcription process causing important chromosomal aberration (IARC, 1982).

### **2.1.2. Lead**

Among toxic heavy metals, a naturally occurring bluish-gray metal was known as Lead (Pb). Although it could be found in all parts of our environment most of it is in human activities including manufacturing, mining, and burning fossil fuels. Lead (Pb) has an atomic number of 82

and atomic mass of 207. It is the heaviest non-radioactive metal that naturally occurs in substantial amounts in the earth's crust. Pb is the most common among the heavy metals and its most abundant isotope is <sup>208</sup>Pb. Other stable lead isotopes also exist (Biernacka *et al.*, 2006). It is one of the major heavy metal and considered as an environmental pollutant.

Lead is used in the production of batteries. It was probably the more common metal that is associated with heavy metal poisoning and toxicity. All the recent news about the presence of lead in kids' toys has helped create public awareness about the dangerous effects of lead. Throughout the world in every year the industry produces about 2.5 million tons of lead mostly used for batteries. This metal forms complexes with Oxo-groups in enzymes to affect virtually all steps in the process of hemoglobin synthesis and porphyria metabolism (Schumann, K. 1990). Toxic levels of lead in human have been associated with encephalopathy, seizures and mental retardation (Kasuya, M. et al., 1992).

### **2.1.3. Cadmium**

Cadmium was one among toxic heavy metals and found in all rocks and soils, including mineral fertilizers and coal contain. This metal does not corrode easily called novel metal and have many uses including: batteries, metal coatings, pigments and plastics. Further, it was used in PVC plastics, nickel-cadmium batteries, and paint pigments. It could also be found in soils because fungicides, insecticides, sludge, and commercial fertilizers that use cadmium are used in agriculture. The most severe form of Cd toxicity in humans is "itai-itai", a disease characterized by excruciating pain in the bone (Yasuda, M. et al., 1995). Other health implications of Cd in humans include kidney dysfunction, hepatic damage and hypertension. However, it has been suggested that overall nutritional status (rather than mere Cd content of food) is a more critical factor in determining Cd exposure. There are also other heavy metals which are considered toxic, but the researcher's intention was focused on lead (II) ions only due to the absence of lamp for other metals in our university.

## 2.2. Current Heavy Metal Ions Removal Technologies

Several treatment technologies are available to reduce the pollutants' concentrations in water and wastewater, including chemical oxidation and reduction, membrane separation, liquid extraction, ion exchange, electrolytic treatment, electroprecipitation, coagulation, flotation, evaporation, hydroxide and sulfide precipitation, crystallization, ultrafiltration, and electrodialysis (Fu and Wang, 2011; Gupta and Ali, 2013) which differ in their effectiveness and cost. Several researches have compared different physico-chemical treatment methods for water and wastewater treatment (Keng et al., 2013). Among various treatment technologies, adsorption using activated carbon has been considered as one of the best alternative treatments for water and wastewater treatment due to its high removal efficiency without the production of harmful by-products (Bhatnagar et al., 2013; Fu and Wang, 2011; Gupta and Ali, 2013; Keng et al., 2013).

In the 1940's, activated carbon was introduced for the first time as the water industry's main standard adsorbent for the reclamation of municipal and industrial wastewater to a potable water quality (Kurniawan et al., 2006). It has been found as a versatile adsorbent due to its high capacity towards various pollutants because of high surface area and well developed porous structure. Production of activated carbon is relatively complicated and involves carbonization and activation stages. In spite of this, activated carbon could not be used as adsorbent for large scale water treatment in poor or developing countries due to its high cost of production.

Moreover, the regeneration of activated carbon is difficult due to the use of expensive chemicals, high temperatures, and hence, its regeneration is not easily possible on a commercial scale. The use of low-cost adsorbents has been investigated as an alternative for current expensive methods for the removal of pollutants from aqueous solutions. Various approaches (e.g. use of microorganisms to detoxify the metals by valence transformation, extracellular chemical precipitation, or volatilization, nanomaterial's mixed with natural sorbent) have been studied for the development of cheaper and more effective technologies, both to decrease the amount of wastewater produced and to improve the quality of the treated effluent (Babel and Kurniawan, 2003). Nano sized metal oxides are used as the novel adsorbent to remove heavy metal ions in

wastewater due to their higher efficiency (higher surface areas) and faster kinetics (intraparticle diffusion) (Luciano Carlos, et al., 2013).

### **2.3. Applications of Nanoscale materials in Heavy Metal ions Removal**

Nanostructure science and technology is a broad and interdisciplinary area of research and development activity that has been growing explosively worldwide. It is a field focused on the design, synthesis, characterization and application of various materials and devices on the nanoscale. Nanoscale materials are defined as a set of substances where at least one dimension is less than approximately 100 nanometers. It is already having a significant commercial impact, which will increase in the future having the potential for great impacts in electronics, biomedical, energy, environment, etc.(Mansoori *et al.*, 2008; S. Mondal, 2017).

As the exciting field of nanotechnology develops, the broader environmental impacts of nanotechnology will also need to be considered. Such considerations might include: the environmental implications of the cost, size and availability of advanced technological devices; models to determine potential benefits of reduction or prevention of pollutants from environmental sources. Pollution prevention by nanotechnology refers on the one hand to a reduction in the use of raw materials, water or other resources and the elimination or reduction of waste and on the other hand to more efficient use of energy or involvement in energy production (USEPAR, 2007).

#### **2.3.1. Multi Component Nano-Sorbents**

Dimensional stability, chemical resistance, mechanical properties, decreased permeability to gases, surface appearance etc are the properties that reinforce the general behavior of nanocomposite towards their considerable enhancement. Alumina,  $Al_2O_3$  is one of the most useful oxide ceramics, as it has been used in many fields of engineering such as coatings, heat-resistant materials and advanced ceramics. This is due to it is hard, highly resistant towards bases and acids, allows very high temperature applications and have excellent wear resistance. Furthermore, it was as well used in heterogeneous catalysis because it is thermally stable and permits the dispersion of energetic phases due to its high specific surface area. Similarly,  $Fe_2O_3$  (hematite) nanomaterials have been studied, including their shape-specific properties, synthesis

methods and potential applications in catalysis, adsorption and field emission etc. Recently, many relative research works has been reported by using an efficient and sufficiently practical methodology to prepare such composites, as those based on magnetic iron oxides, particularly those involving combustion synthesis to prepare alumina /iron oxide nanocomposite materials. This type of synthesis is characterized by highly exothermic reaction with temperature ranging from 400-600°C (Chandan, B. P., 2008). Multi component sorbents comprising of mixtures of metal oxides, clay, quartz and organic compounds are ubiquitous in soils and aquatic environments and have been shown to be significant in determining the environmental distribution of various contaminants and nutrients (Xu, Y., Axe, L. 2005).

The physico-chemical properties of these multi component sorbents differ significantly from those of their single component constituents indicated by characterization studies (Rodic, D., et al., 2001). It was this difference in physico-chemical properties that are believed to be primary reason for differences in sorption behavior between multi-component and single component solids. For example, (Agbenin, J.O., 2003) attributed increase Ni adsorption in a Fe-oxide/silica multi-component system (compared to a silica only system) to increases in surface area, porosity and surface charge distribution.

Mixed Al-Fe hydr(oxide) are among the most significant multi-component sorbents. In addition to being ever-present in soil and aquatic environments, where they occur as coatings on other particles or as discrete solids, mixed Al-Fe hydr(oxides) have high specific surface areas and surface functional groups capable of interacting with both cationic and anionic species. Although sorption characteristics of single-component Al or Fe hydr(oxides) have been widely studied.

Currently, many studies have shown that in both soils and aquatic environments Al and Fe-hydr(oxides) often control the biogeochemical cycling of nutrients, such as phosphate, via colloidal transport and/oradsorption/desorption mechanisms. Since, naturally occurring oxides are typically co precipitated mixtures; it was reasonable to postulate that co-precipitated mixed metal Al-Fe hydroxides are likely to play a major role in the geochemical cycling of nutrients and contaminants (Wang J.L. and ChenC.,2006).An aqueous solution of a redox system constituted by the nitrate ions of the metal precursor, acting as oxidizer and a fuel like citric acid method or many others was heated up to moderate temperatures and upon dehydration, the

strongly exothermic redox reaction develops and provides an energy for the formation of the oxide.

## 2.4. Adsorption

A process occurs when a gas or liquid solute accumulates on the surface of a solid or a liquid (adsorbent), forming a molecular or atomic film (the adsorbate) was known as adsorption. It is not similar to absorption, in which a substance diffuses into a liquid or solid to form a solution, but sorption is the activities that encompasses both processes and desorption was the reverse process of sorption.

Particle size of adsorbent affinity of the solute for the adsorbent, surface area of adsorbent, degree of ionization of the adsorbate molecule (more highly ionized molecules are adsorbed to a smaller degree than neutral molecules), pH etc. were considered as the most important factors affecting the adsorption process.

### 2.4.1. Fundamentals of Adsorption

Adsorption was continuing until equilibrium will be established between the substance in solution and the same substance in the adsorbed state. At equilibrium a relationship exists between the concentration of the species in solution and the concentration of the same species in the adsorbed state. Here, adsorption equilibrium was the equilibrium upon contacting the amount of adsorbent with a wastewater containing an adsorbable substance adsorption would take place. The quantity of adsorbed metal ions was calculated by the difference of the initial and equilibrium amounts of metal ions in solution divided by the weight of the adsorbent. The adsorbate in the glass ware is calculated from mass balance as follow:

$$m (q - q_e) = (C_0 - C_e)v \quad (1)$$

From which a relationship between values of C and the corresponding equilibrium value of q can be established. To determine equilibrium relationship at  $q_0 = 0$ ,

$$q_e = \frac{v}{m} * (C_0 - C_e) \quad (2)$$

Where,  $v$  is the volume of liquid,  $m$  is the mass of adsorbent used,  $C_0$  is the initial, and  $C_e$  is the adsorbate residual concentration in solution.

Here, we speak the basic difference between adsorption and absorption clearly. Adsorption was a mass transfer process in which substances present in a liquid phase are accumulated on a solid phase and thus removed from the liquid. Whereas absorption is a process in which the molecules are accumulated in the phase. In absorption process the molecules are accumulated in the phase whereas in adsorption the accumulation takes place at the boundary layer between solid and liquid phase. The solid phase onto whose surface the target compound is adsorbed was referred to as the adsorbent and the target compound (e.g., metal ions) is called the adsorbate (Kummel, R. and E. Worch, 1990). During the adsorption process; dissolved species are transported into the porous adsorbent particle by diffusion and are then adsorbed onto the extensive inner surface of the adsorbent. For a detailed overview of adsorption theory, the studies of (John, C., et al., 2005) are recommended.

On the basis of the interaction between adsorbate and adsorbent surface, chemisorptions and physisorption can be identified. In chemisorption the adsorbate reacts with the surface to form a covalent or an ionic bond. Physisorption is a rapid process caused by nonspecific binding mechanisms such as van der Waals forces and results in bonding energies of 4 - 40 kJ/mol. Generally, physical adsorption is less specific for which compounds adsorbed to surface sites, has weaker forces and energies of bonding, operates over longer distances (multiple layers) and is more reversible (John, C., et al., 2005).

In contrast to the adsorption of organic adsorbates from water (polar solvent) onto a nonpolar adsorbent (activated carbon), where vanderwaals forces are predominating, adsorption of ionic species (e.g., metal ions) onto iron oxide surfaces is mostly driven by electrostatic attraction, which is highly dependent on pH and ionic strength. The affinity of the adsorbate for an adsorbent is quantified using adsorption isotherms, which are used to describe the amount of adsorbate that can be adsorbed onto an adsorbent at equilibrium and are usually a function of the liquid phase concentration. To develop isotherms, a known amount of adsorbate in a constant volume of liquid is used to different adsorbent dosages. Here, we consider the difference between adsorption of a single and of multiple compounds. In the latter case, the different adsorbates were competing for adsorption sites and the adsorption equilibrium as well as the isotherm can be significantly

different than without competition. In a multi-component system, the initial concentration of the target adsorbate influences the resultant isotherm. In order to describe the adsorption equilibrium mathematically, different models exist, differing in complexity and in the number of parameters necessary. Of practical importance are mainly two-parametric isotherms, in particular those formulated by (Freundlich, H., 1906, Langmuir, I., 1918).

### 2.4.2. Langmuir adsorption isotherm

The theoretical Langmuir isotherm was valid for sorption of a solute from a liquid solution as monolayer adsorption (Langmuir, I., 1918) on a surface containing a finite number of identical sites. The equilibrium between surface and solution as a reversible chemical equilibrium between species was described by using this model. It assumes uniform energies of adsorption onto the surface without interaction of adsorbate in the plane of the surface where adsorbate molecules can be chemically bound. The Langmuir equation assumes that all adsorption sites are energetically equal. That is why the Langmuir equation is in most cases only applicable for small concentration ranges.  $R_L$  indicates the isotherm shape and whether the adsorption is favorable or not. The Langmuir nonlinear equation is commonly expressed as follows (Langmuir, I., 1918):

$$q_e = Q_o \frac{C_e}{1+bC_e} \quad (3)$$

To derive the model parameters  $Q_o$  and  $b$ , equation 3 can be linearized. The linear Langmuir isotherm allows the calculation of adsorption capacities and is equated by the following equation.

$$\frac{C_e}{q_e} = \frac{1}{bQ_o} + \frac{C_e}{Q_o} \quad (4)$$

The essential characteristics of a Langmuir isotherm can be expressed in terms of a dimensionless constant separation factor or equilibrium parameter  $R_L$ , which is defined by:

$$R_L = \frac{1}{1+bC_o} \quad (5)$$

For all the above equation (1-5),  $C_o$  was the initial adsorbate concentration in solution (mg/L),  $C_e$  was the adsorbate residual concentration in solution,  $q_o$  was the initial amount of adsorbate per unit mass of adsorbent (mg/g),  $m$  was mass of adsorbent (g) and  $v$  is the volume of liquid,  $q_e$  is milligrams of adsorbate accumulated per gram of the adsorbent material,  $Q_o$  is the maximum uptake corresponding to the site saturation and  $b$  is the ratio of adsorption and desorption rates.

Table 1: Type of isotherm for various  $R_L$ .

$R_L$	Type of isotherm
$R_L > 1$	Unfavorable
$R_L = 1$	Linear
$0 < R_L < 1$	Favorable
$R_L=0$	irreversible

### 2.4.3. Freundlich adsorption isotherm

The Freundlich isotherm can be derived assuming a logarithmic decrease in the enthalpy of sorption with the increase in the fraction of occupied sites. Its equation is an empirical expression that encompasses the heterogeneity of the surface and the exponential distribution of sites and their energies and improved to describe adsorption in aqueous solutions than the Langmuir isotherm. Also its equation can only be used to describe experimental data within a limited concentration range where the constants are valid. The ideal adsorbed solution theory (IAST) has been developed for multi-component adsorption, which describes multi-component equilibria based on single-solute isotherms. This model is commonly given by the non-linear equation (Freundlich, H., 1906):

$$q_e = K_f C_e^{1/n} \quad (6)$$

Where  $K_f$  is the adsorption or distribution coefficient and represents the quantity of adsorbate adsorbed onto adsorbent for unit equilibrium concentration and called a constant for the system related to the bonding energy.  $1/n$  is an empirical constant describes the magnitude of the adsorption driving force onto the sorbent. If its value gets closer to zero, then it becomes more heterogeneous. Batch experiments, using logarithmic equation of the data and the linearized form of the Freundlich equation to determine both  $K_f$  and  $n$  were given by (Sairam *et al.*, 2009):

$$\text{Log } q_e = \text{log } K_f + \frac{1}{n} \text{log } C_e \quad (7)$$

### 2.5. Kinetics of Adsorption

Kinetics of adsorption gives information about the prediction of adsorption rates and modeling of the processes. Its parameters describe how fast the adsorbate adsorbed onto adsorbent surfaces. Successful application of the adsorption demands innovation of cheap, easily available and

abundant adsorbents of known kinetic parameters and sorption characteristics. Till now, several kinetic models (pseudo first- and second-order equations, intra-particle diffusion and Elovich equations) are used to interpret the time dependent experimental data and examine the controlling mechanism of adsorption process (Rodrigues, L.A. and M.C.P. Silva, 2009, Buzuayehu Abebe, et al., 2017). The Pseudo-first order model (Hamdaoui, O. and M. Chiha, 2007) is given as:

$$\log(q_e - q_t) = \log Q_e - \frac{K_1 t}{2.303} \quad (8)$$

The pseudo-second-order kinetic model equation (Ho and McKay, 1998) is given as,

$$\frac{t}{q_t} = \frac{1}{K_2 q_e^2} + \frac{t}{q_e} \quad (9)$$

Half-adsorption time,  $t_{1/2}$ , is defined as the time required for the adsorption to take up half as much adsorbate as its equilibrium value. This time is often used as a measure of the adsorption rate:

$$t_{1/2} = \frac{1}{K_2 q_e} \quad (10)$$

The Elovich equation is given as follows (Gunayet *al.*, 2007).

$$\frac{dq_t}{dt} = \alpha \exp(-\beta q_t) \quad (11)$$

To simplify the Elovich equation, it is assumed that  $\alpha \beta t \ll 1$  and by applying the boundary conditions  $q_t = 0$  at  $t = 0$ , this equation becomes

$$q_t = \alpha \ln(\alpha \beta) + \beta \ln t \quad (12)$$

Thus, the constants can be obtained from the slope and intercept of a straight line by plotting of  $q_t$  versus  $\ln t$ . The intra-particle diffusion equation (Chien and Clayton, 1980) can be written as;

$$q_t = k_i t^{1/2} + C \quad (13)$$

## 2.6. Thermodynamic of Adsorption

The spontaneity of the adsorption processes was easily determined by obtaining information from thermodynamics concept. Therefore, one can understand the concept of Gibb's free energy change ( $\Delta G$ ) to determine a given process is whether spontaneous or non-spontaneous. If the value of  $\Delta G$  is negative, then the reactions occur spontaneously at a given temperature.

The thermodynamic parameters such as change in standard free energy ( $\Delta G$ ), enthalpy ( $\Delta H$ ) and entropy ( $\Delta S$ ) can be calculated by using the following equation (Rodrigues and Silva, 2009):

$$\Delta G = -nRT \ln K_c \quad (14)$$

$$\ln K_c = -\Delta H^0/RT + \Delta S^0/R \quad (15)$$

$$\Delta G^0 = \Delta H^0 - T\Delta S^0 \quad (16)$$

Where R (8.314 J/molK) is the gas constant, T (K) is the absolute temperature and  $K_c$  is the standard thermodynamic equilibrium constant defined by  $q_e/C_e$ . By plotting the graph of  $\ln K_c$  versus  $T^{-1}$ , the value of  $\Delta H^0$  and  $\Delta S^0$  can be estimated from the slopes and intercept, respectively.

## 2.7. Regeneration

Regeneration of used adsorbents is a process of getting again the used adsorbents through desorption process. If adsorption is thought of as surface complexation reaction a high concentration of  $H^+$  ions shifts the equilibrium so that less adsorbate (metal ions) is bound to the surface. In addition to this, the surface acid/base reaction is shifted more towards positively charged species, which hinders adsorption of cations such as metal ions. As a result, a pH decreases due to the use of HCl, shifts the adsorption equilibrium and can result in desorption of the adsorbate. If the adsorption capacity can be regained in this process, the adsorbent was regenerated. In many studies, hydrochloric acid (HCl) solution has been shown as suitable regenerant for metal oxide adsorbents as well as hybrid anion exchange resins. The metal ions desorbability was defined as:

$$\% \text{ desorption efficiency} = \text{Desorbed/Adsorbed} * 100 \quad (17)$$

Where,

Desorbed: the concentration of the metal ions after the desorption process

Adsorbed:  $(C_o - C_e)$  for each recovery process.

## **3. MATERIAL AND METHODS**

### **3.1. Experimental Site**

#### **3.1.1 Apparatus and Instruments**

Synthesis of the adsorbent, the batch adsorption experiments and (Atomic Absorption spectrophotometer, AAS, Pg Instrument ASS500F, S/N 20-0930-21-0020, power 150W) were carried out at the Applied Chemistry Department, laboratory, Adama Science and Technology University (ASTU). Rotary shaker (Orbital shaker SO1 made in UK) was used for equilibrium reaction. XRD characterizations of the synthesized adsorbent and (FTIR, Bruker IFS 120 M, PerkinElmer) study was done at Addis Ababa University, Addis Ababa, Ethiopia. SEM (S4800, Hitachi Corporation, Japan) and EDX ((JEM-2100, JEOL, Japan) characterization was done in India. Hot air oven (Contherm260 M and Furnace BIBBY Stuart, UK), were used in various measurements to generate the required analytical data. The laboratory apparatuses that were used during the study included different sized glass wares (Beaker, Volumetric & Erlenmeyer flasks, Cylinders, Pipettes, Dropper and Funnels), Crucible dish, Filter paper, Mortar & Pestle and Sieve (250  $\mu\text{m}$ ).

#### **3.1.2. Chemicals and Reagents**

Analytical grade  $\text{Fe}(\text{NO}_3)_3 \cdot 9\text{H}_2\text{O}$  (98%, BDH chemicals Ltd, England) and  $\text{Al}(\text{NO}_3)_3 \cdot 9\text{H}_2\text{O}$  (95% E. Merck) were used for synthesis of the sorbent.  $\text{Pb}(\text{NO}_3)_2$  (99% CDH Laboratory reagents), HCl solutions,  $\text{HNO}_3$ , sodium borohydride and all the reagents were used for the experiments.

### **3.2. Experimental Procedure**

#### **3.2.1. Collection and Preparation of Maize Cob (MC)**

Maize cobs (MC) sample was collected from Sile Sira local farm and cut into small pieces and washed several times with deionized water. Afterwards, they were dried under vacuum in a desiccator at room temperature (25<sup>0</sup>C), and then it was milled and sieved through a no. 400  $\mu\text{m}$ .

Then the powdered was stored in plastic container until to use in the experiment (Tellez *et al.*, 2011).

### **3.2.2. Synthesis of Nano-Sized Mixed Oxide**

To synthesize nano sized oxide-layered traditional sorbent impregnation method was used as adapted by (Buzuayehu Abebe *et al.*, 2017). To this effect, 0.1 M nano sized Fe-Al binary mixed oxide was prepared by impregnating aluminum and iron nitrate aqueous solution together with 90 % iron nitrate aqueous solution and 10 % aluminum nitrate aqueous solution and dried at 110°C in an oven over night (Dong, X., H. Zou and W. Lin, 2006).

### **3.2.3. Synthesis of nano-sized mixed oxide/natural sorbent**

Maize cobs (MC) collected from local farm were cut into small pieces, washed several times with water and air-dried. Then the substrates will be grounded to small particle sizes (< 850 µm and powdered form) and finally it was kept in plastic containers for subsequent use as precursor. Next, a mixture of 2.4 g Maize cobs (MC) powder impregnated with 1.39 g of Fe-Al binary mixed oxide were dissolved in 100 mL deionized water and stirred with 30 min while 0.01 M sodium borohydride was added dropwise. Afterwards, the mixture were stirred for an additional 30 min, filtered, washed five times in ethanol, and dried at room temperature for 48 h in a desiccator (Tellez *et al.*, 2011). Further it was calcined at different temperatures of (400°C and 600 °C) to see the temperature effect of mixed oxides and MC adsorbents (ICCEA, 2012).

### **3.3. Characterization of the as-synthesized powder (solid-phase characterization)**

The size of the primary crystallite ( $D_s$ ) of the solid-phase was calculated from the XRD diffractograms according to the DubyeScherrer equation:  $D_s = 0.9\lambda / \beta \cos\theta$  (Johnston *et al.*, 2002). Where,  $D_s$  is mean crystallite size (nm),  $\lambda$  wavelength of the incident radiation ( $\lambda = 0.15405$  nm),  $\beta$  pure diffraction broadening (radians) and  $\theta$  is the Bragg angle (degrees, half-scattering angle). Usually,  $\beta$  was taken as the full width at half maximum of the major diffraction band (FWHM). The XRD, pattern was obtained through a Cu target  $K\alpha$  radiation. For farther composition identification and structural elucidation was done using FT-IR, SEM and EDX.

### **3.4. Wastewater Sample Collection and Digestion**

Wastewater samples were collected from different points in Modjo River by using pretreated plastic bottle. Sampling was carried out across the seasons in the study area from April-June 2017. Before to this, the plastic-bottles were rinsed with 0.02M HNO<sub>3</sub> to maintain the constant pH and minimize loss of sample because of variation in PH, evaporation, precipitation and other relevant physical and chemical properties(EPA Guidelines, 2007). Modjo River was found in Mojo (also transliterated as Modjo) which is a town in central Ethiopia, named after the nearby Modjo River. Located in the Misraq Shewa Zone of the Oromia Region, it has a latitude and longitude of 8° 39' N 39° 5' E with an elevation between 1788 and 1825 meters above sea level. It is the administrative center of Lome woreda. This river is considered as the most polluted river because of the increased industrialization near to Modjo town including leather industry, textile industry, etc.

The digestion procedure for Wastewater was carried out by transferring a measured volume of 50 mL of well mixed acid preserved water sample into a flask. Then 1 mL of conc. HNO<sub>3</sub> and 0.5 mL of HCl were added into the flask. Then followed a few boiling chips were added into the flask. The mixture were boiled and evaporated on a hot plate to the lowest volume possible (10 to 20 mL). Continue heating and adding conc. HNO<sub>3</sub> as necessary until digestion is complete as shown by a light color clear solution. Do not let sample dry during digestion. After this the flask were wash down with water and filtered. Then the filtrate was transferred into 10 mL volumetric flask with two 5mL portions of water, adding these rinsing to the volumetric flask and cooled and diluted to the mark and mixed thoroughly. The digested wastewater was ready to batch adsorption studies (U.S EPA Method 2002).

#### **3.4.1. Stock solutions of metal ions**

Stock solutions were prepared in doubled distilled water (DDW) from the salts of Pb (II) ions under investigation. For 1000 mg/L solution preparation, dried salts of 1.598g of Pb(NO<sub>3</sub>)<sub>2</sub> was dissolved in 1000 mL of DDW. The resulting stock solution was stored in volumetric flasks (Panneerselvam *et al.*, 2011).

### 3.5. Adsorption studies

Adsorption studies were performed by determining different factors that affecting the sorption parameters (solution pH, adsorbent dose, contact time, agitation speed and initial adsorbate concentration). Each parameter influence on the Pb (II) ions adsorption was determined by keeping other parameters at constant and optimized value. Thus, the influence of solution pH was carried out by adding 2 g of the adsorbent into 250 mL Erlenmeyer flask containing 10 mg/L of Pb (II) ions solution by varying pH of the solutions to 2, 4, 6, 8 and 9 and the effect of adsorbent dose was carried out by varying the amount as 0.04, 0.08, 0.16, 0.3, 0.5, 1, 2 g and 2.5 g. Following this, the effect of contact time was determined by varying the period as 3, 7, 9, 18, and 24 hours and the effect of agitation speed of metal ion adsorption was also determined, by varying the agitation speed as, 100, 150, 200, 250 and 300 rpm. Finally, the effect of initial adsorbate concentration was carried out using different initial metal ion concentrations of 10, 20, 30, 50, and 100 mg/L. All the above experiments were evaluated by placing in different 500 mL Erlenmeyer flasks. During the experiment, the flasks was stoppered and continuously shaken. And then at the end of the adsorption period the solution will be filtered and analyzed for metal ion equilibrium concentration. For all the above parameters percent of adsorption (%) was calculated using the following equation:

$$\text{Percent of adsorption (\%)} = \frac{C_0 - C_e}{C_0} * 100\% \dots (2)$$

where:  $C_0$  = the initial concentrations (mg/L) and  $C_e$  = equilibrium concentrations (mg/L) of the lead ion.

#### 3.6.1. Adsorption isotherms

The affinity of the adsorbate for an adsorbent was quantified using adsorption isotherms, which are used to describe the amount of adsorbate that can be adsorbed onto an adsorbent at equilibrium and are usually as a function of the liquid phase concentration. For this both Freundlich and Langmuir models (Langmuir, I., 1918; Freundlich, H., 1906) were employed to describe the experimental results of metal ion adsorption. Metal ion adsorption isotherms were determined by keeping all parameters at optimized conditions. Initial metal ions concentration was varied from 10-250 mg/L. In separate flask 25 mL of solutions containing different amounts

of metal ion concentration was added. After the reaction period, all samples were filtered of and analyzed for the corresponding metal ion concentration.

### **3.6.2. Kinetics of adsorption**

Effect of metal ion adsorption kinetics was determined by varying the contact time as; 1, 2, 4, 6, 8, 10 and 12 hrs by keeping all parameters (pH, adsorbent dose, contact time, agitation speed and initial Pb (II) ions concentration) at optimized value.

### **3.6.3 Thermodynamics of adsorption**

Thermodynamics of adsorption gives information whether the processes are spontaneous or not at a given temperature (A. Olgun et al., 2013). Therefore, in order to determine the effect of temperature on sorption phenomenon, all predetermined and optimized values of parameters (pH, dosage, contact time, speed of agitation and concentration) was used and the temperature was established at 30-60°C.

### **3.6.4. Desorption of Metal ion**

Pb (II) ions desorption was studied using Pb (II) ions loaded powder sample. The optimized amount of adsorbent loaded powder (2 g) was added into each flask containing 25 mL of deionized water and 0.1 M NaOH and 0.1 M HCl solutions was used to adjust pH of the solution from 2-9. The solutions were agitated at optimized value. Then filtered and analyzed for metal ion concentration according to the method described by (O.R. Harvey, R.D. Rhue, 2008). The quantity of desorbed metal ion was determined by the amount of metal ion in the solution after each desorption experiment was performed. Through this process we regenerate the adsorbent used to adsorb the metal ions throughout the experiments.

## 4. RESULTS AND DISCUSSION

### 4.1. Synthesis and Characterization

#### 4.1.1. X-ray diffraction (XRD)

The XRD pattern shows relatively hematite peaks (Figure 2). Since, most of the structure was dominated by  $\text{Fe}_2\text{O}_3$  than  $\text{Al}_2\text{O}_3$  and MC. This could be due to the presence of the small percentage of  $\text{Al}_2\text{O}_3$  and MC in the composite adsorbent. Sample with the smallest crystallite size was selected from the obtained XRD result using Debye Scherer's equation and used for further adsorption studies. Relatively, composite sample (A) calcined at  $400^\circ\text{C}$  has small particle size (22.71 nm) than sample (B) calcined at  $600^\circ\text{C}$  whose crystalline size was 22.86 nm. This is possibly due to little temperature effect; as calcinations temperature increases, the crystal size increases insignificantly. The XRD peaks for both data,  $2\theta$  values represented as miller indices (111), (220), (311), (400), (422) and (440) shows all the hematite peaks (Figure 2). It has also been observed from the XRD patterns (Figure 2) that there is no significant change in the structure of the sorbent materials at different calcination temperatures of  $400^\circ\text{C}$  and  $600^\circ\text{C}$ . In addition, the absence of sharp peaks, confirms more of amorphous nature of the sorbent than crystalline nature.

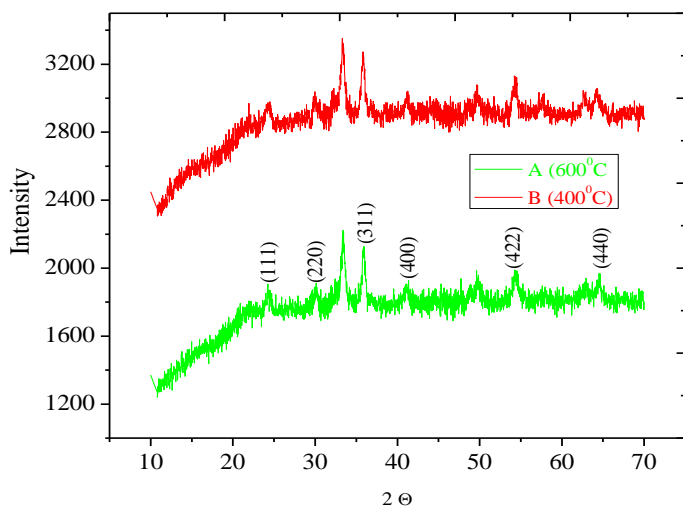


Figure 2. XRD pattern of as synthesized powders, when sample code A and B calcined at  $600^\circ\text{C}$  and  $400^\circ\text{C}$  respectively.

#### 4.1.2. Scanning Electron Microscope (SEM) and EDX Analysis

Here it is possible to state the usefulness of Scanning Electron Microscopy (SEM). SEM was commonly used to study morphologies, structures, surfaces and forms of materials. SEM images with different magnifications and different areas of the sorbent system were shown in (Figure 3). It was observed that Fe-Al-MC sorbent exhibit variation in surface morphologies and was shaped like a flat material, with a slightly rough surface and amorphous structure. The presences of all the elements were confirmed by EDX analysis (Figure.3). As we can see from Figure 3), the Fe-Al-MC was mainly composed of the elements C, O, Fe, and Al, and this further illustrated that the adsorbent had been synthesized successfully. In line with this, (J. Sun et al., 2018) reported a research on  $\text{Fe}_3\text{O}_4/\text{MgAl}$ -layered double hydroxide adsorbent mainly composed C, Ca, Fe, Mg, O and Al. The purities of Fe, O and C were higher than those of Al. This is because the Fe-Al-MC had many functional groups that contained C and O and the higher percentage of Fe portion used in the synthesis. This variation indicates that the heterogeneity of the nano sorbent system.

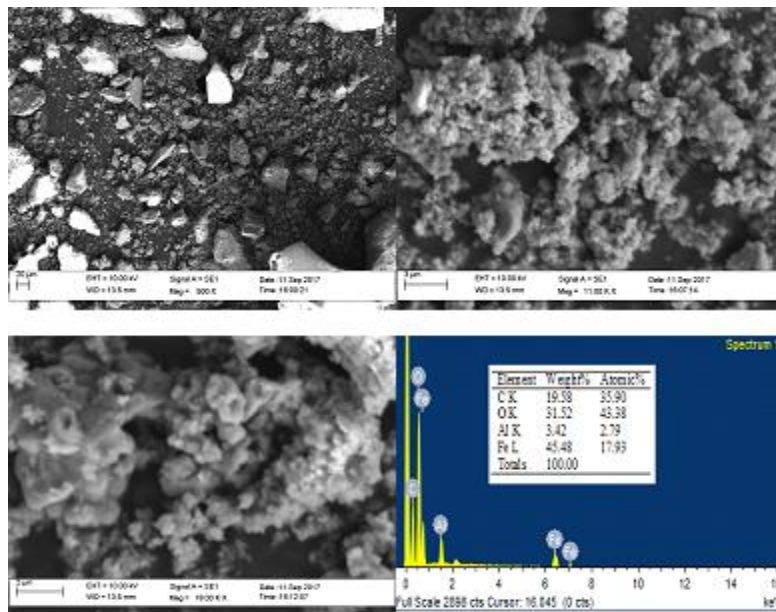


Figure 3. SEM micrographs with EDX analyses of NP-MC sorbent system.

### 4.1.3. Infrared Spectroscopic Studies

In order to have information about the interaction between aqueous heavy metal ions and solid nano sized oxides mixed with maize cob sorbent system, FT-IR technique was employed.

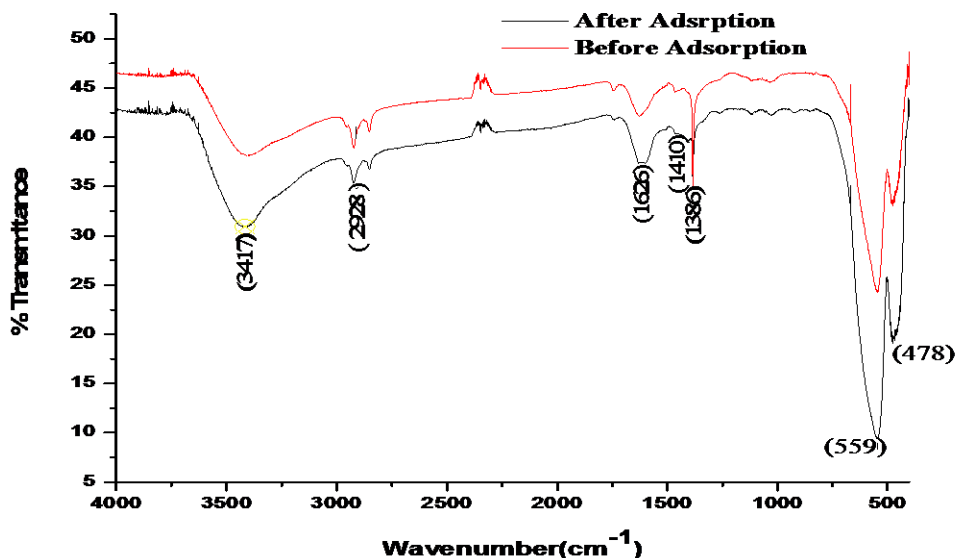


Figure 4. FT-IR Spectrum of nano sized oxide mixed with MC sorbent. FT-IR spectra of NP-MC sorbent before and after adsorption were shown (Figure.4). Here, we observed the strong alkyl C-H stretch bands nearly around  $2928\text{ cm}^{-1}$  due to C-H bonds in the  $\text{CH}_2$  and  $\text{CH}_3$  groups. The peak at  $1386\text{ cm}^{-1}$  before adsorption was due to the CO single bond and the broad band centered in the range of  $3417\text{ cm}^{-1}$  after adsorption is caused by the presence of the hydroxyl functional group (OH) or it may corresponds to OH stretching frequency of  $\text{AlO}(\text{OH})$  phase as suggested by Chandan, (Chandan, B.P., 2008). According to (Zhang *et al.*, 2007), a band at  $1626\text{ cm}^{-1}$  primarily recognized to the bending vibration of hydroxyl groups of iron (hydr) oxides (Fe-OH) and the band spectrum in the region around  $478\text{ cm}^{-1}$  shows the presence of mixed metal oxides with MC bond in specific vibration and the adsorption band at  $559\text{ cm}^{-1}$  shows the presence of hematite.

From the graph we understood that, the availability of more  $\text{H}_2\text{O}$  molecules during experiment processing shows relatively higher strengths of the peaks after adsorption than before adsorption. While before adsorption, since the adsorbent were calcined there is no more  $\text{H}_2\text{O}$  molecules expected. After adsorption new peak appeared at  $1410\text{ cm}^{-1}$  which is bending vibration of

adsorbed lead (Liu *et al.*, 2008) and corresponds to adsorbed water of adsorbents. This is because of replacement reaction carried out in the process (surface hydroxyl groups were replaced by the adsorbed lead). The band shifting from  $3417\text{ cm}^{-1}$ ,  $2928\text{ cm}^{-1}$ , and  $1626\text{ cm}^{-1}$  on the mixed hybrid adsorbent before and after adsorption corresponding to the bonded OH stretching,  $-\text{CH}_2-$  stretching in alkene and  $-\text{C}-\text{O}-\text{C}-$  stretching has revealed the successful binding of MC with NP to form NP-MC. The peak at  $559\text{ cm}^{-1}$  assigned to Fe-O group on NP-MC may indicated the presence of NP on the composite (Panneerselvam *et al.*, 2011). This interaction also accounted for the mechanism of surface modification of NP with MC. The IR spectrum of the NP-MC before and after adsorption indicates distinct changes in the absorption intensities of, CO stretch in acids, and OH stretch in alcohols suggesting that such ionizable functional groups on the adsorbent surface are able to bind with the metal ions (Fig.4).

## 4.2. Adsorption Mechanism

The adsorption mechanisms of  $\text{Pb}^{2+}$  ions onto the Fe-Al-MC were investigated as the schematic representation (Figure 5): (Figure 5):

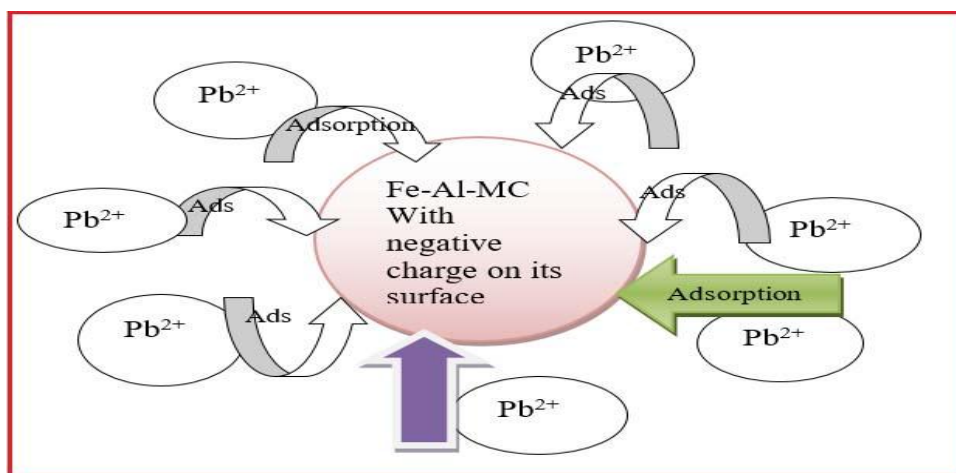


Figure 5. The schematic representation of  $\text{Pb}^{2+}$  ions adsorbed onto the Fe-Al-MC adsorbent.

From the schematic representation for the adsorption mechanisms of  $\text{Pb}^{2+}$  ions onto the Fe-Al-MC adsorbent it is possible to understand that the adsorption mechanisms are dependent on the degree of adsorbate-adsorbent interaction and the adsorbate-solvent interactions. This point view was supported researches reported by (O'Connell, et al., 2008). Therefore, it shows the adsorbate has positive charge and the adsorbent has the negative charge on the surface and the adsorption process enhances greatly.

#### 4.2.1. Effect of pH

The effect of solution pH on the adsorption of Pb (II) ions is demonstrated in the figure 5. The Pb(II) ions removal was evidently dependent on solution pH with relatively greatest adsorption occurring under the conditions of increased solution pH in Fe-Al-MC adsorbent and decreased with decreased solution pH (Figure 6). As the pH of the solution was decreased,  $H^+$  ions competes with  $Pb^{2+}$  ions for the functional groups present on the adsorbent at acidic condition thus lowering the adsorption capacity of the adsorbent (Liu, P., et al., 2014). Generally, to maximize the removal of heavy metals by the adsorbents, knowledge of an optimum pH is important. In addition to this, an increase in pH was found to increase the adsorption efficiency, although to avoid the precipitation of Pb, the pH of the solution was raised only to a maximum value of 6 in this study (Dong C, et al., 2013).

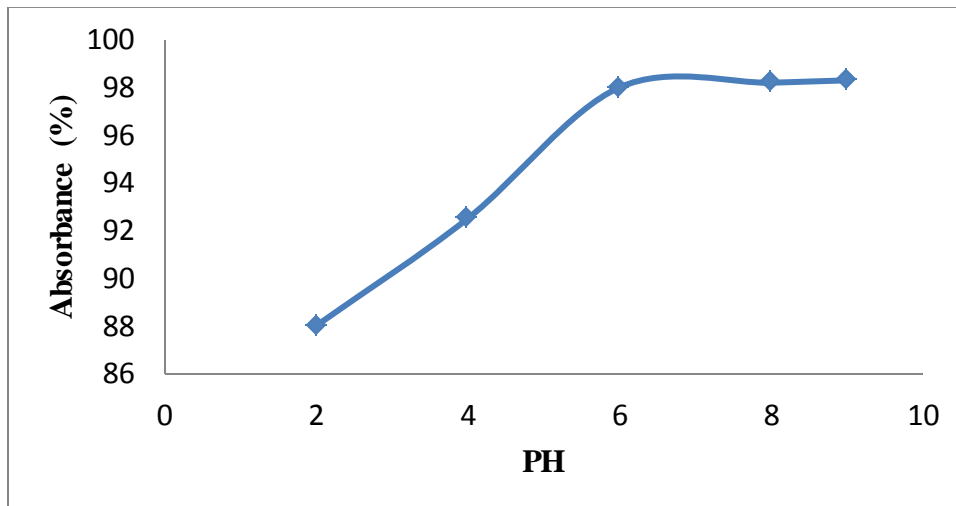


Figure 6. Effect of pH on the removal lead at initial Pb(II) ions concentration ( $C_0 = 10$  mg/L, dose = 2 g, agitation speed = 150 rpm and contact time = 7 h).

#### 4.2.2. Effect of adsorbent dose

The effect of adsorbent dose on the metal ion adsorption capability was determined by varying the amount as 0.04, 0.08, 0.16, 0.3, 0.5, 1.2 and 2.5 g, keeping the pH of solution at the optimized value and concentration, agitation speed and contact time at constant value (agitation speed at 150 rpm, contact time at 7 h and concentration 10 mg/L). Initially the adsorption process was increases, but at higher adsorbent dose it become slow this is b/c at lower adsorbent dose the adsorbate is more easily accessible whereas, at higher adsorbent dose there is a very high

supercritical adsorption onto the adsorbent surfaces that produces a lower solute concentration than when adsorbent dose is low (Figure 7). In line with this, at higher adsorbent dose, the availability of high energy sites decreases with large fraction of lower energy sites being occupied, resulting in lower adsorption capacity but, at the low adsorbent dose, all types of sites are entirely exposed and the adsorption on the surface is saturated faster showing a higher adsorption capacity ( $q_e$ ) (Hadjmohammadi *et al.*, 2011).

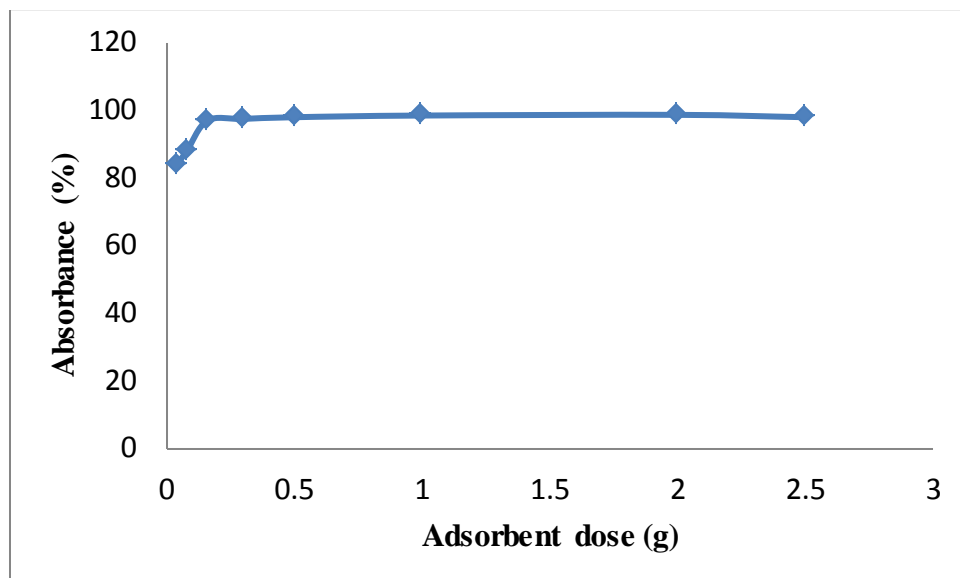


Figure 7. Effect of adsorbent dose on the removal of Pb (II) ions at initial Pb (II) ion concentration 10 mg/L, agitation speed 150 rpm, contact time 7 h and pH at optimized value.

#### 4.2.3. Effect of contact time

The effect of contact time on Pb (II) ions uptake was studied at optimized pH of 6, 2 g dosage and at optimized speed of agitation (150 rpm) and initial Pb II ion concentration (10 mg/L) (Figure 8). Lead (II) ions uptake approached equilibrium faster at contact time of 7 hr because adsorbate generally formed monolayer on the surface of adsorbent. Clearly, the adsorption process could be divided into two steps, a fast step and a slow one. In the first step, the adsorption rate was fast and approximately 98% of the equilibrium adsorption capacity was achieved within the beginning 7 hr. This may also be due to the increased number of vacant sites available at the initial stage. This may be the smaller particle size (22.86 nm) was favorable for the diffusion of Pb (II) ions from bulk solution onto the active sites of the solid

surface of adsorbents. Later on, the process becomes relatively slower due to the intra-particle diffusion was dominated (Satish, *et al.*, 2011).

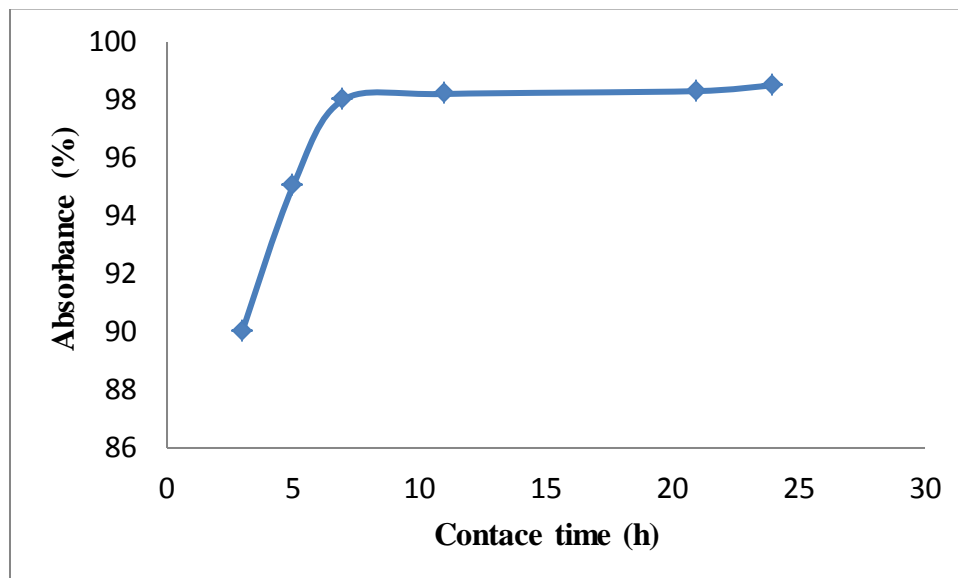


Figure 8. Effect of contact time optimization on the removal of Pb(II) ions (Co = 10 mg/L, pH = 6, adsorbent dose = 2 g and agitation speed = 150 rpm).

#### 4.2.4. Effect of speed of agitation

The effect of agitation speed on adsorption of Pb (II) ions was investigated by varying the agitation speed from 100 to 300 rpm making the initial metal ions concentration constant and at optimized PH. The adsorption efficiency of the adsorbent used in this study was increased as the agitation speed increased from 100 to 150 rpm (97.1% to 99%) (Figure 9), this is owing to the fact that increasing agitation speed could improve the diffusion of solute towards the adsorbent surface. But, beyond this agitation speed the adsorption efficiency decreased because of more agitation speed causes more desorption of Pb (II) ions from the adsorption site in agreement with the work done by (Badmus, *et al.*, 2007, Mansoori, G. A., *et al.*, 2008, Kabbash *et al.*, 2009).

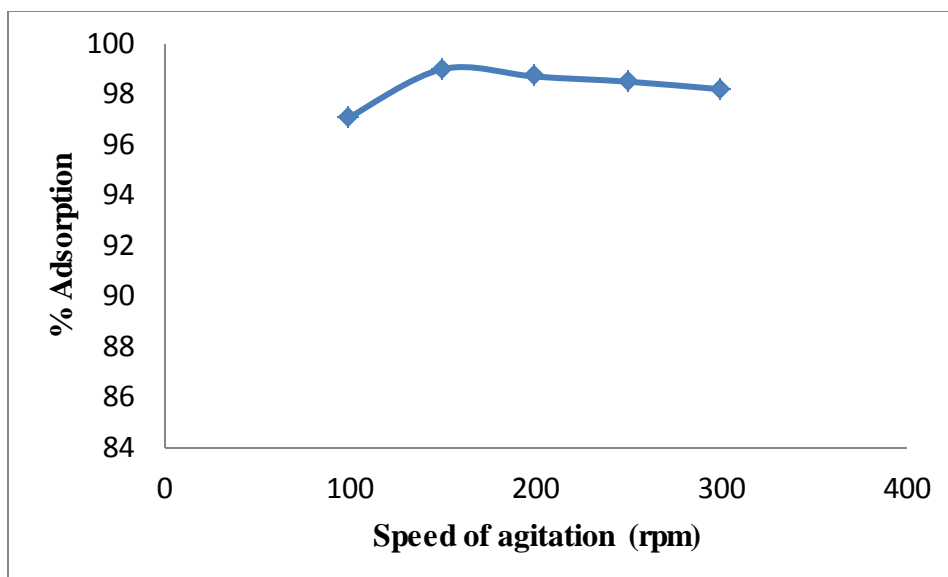


Figure 9. Effect of speed of agitation on the removal of Pb (II) ions (At  $C_0 = 10$  mg/L, pH = 6, adsorbent dose = 2 g and at optimized contact time)

#### 4.2.5. Effect of initial Metal ions concentration

The sorption of metal ions on nanoparticle mixed oxide with MC sorbent system was determined as a function of initial metal ions concentration. The NP-MC adsorbent removal efficiency of the Pb (II) ions was decreased from 99.20% at 10 mg/L to 92% at 150 mg/L (Figure 10). Meaning that, the adsorption efficiency decreases with increasing initial Pb (II) ion concentration (Figure 10). This can be explained by the fact that in case of low concentrations, the ratio of the initial number of moles of solutes to the available surface area of adsorbent is large and subsequently the fractional adsorption becomes independent of initial concentration and consequently higher adsorption yields were obtained. No matter how at higher concentration, most of the adsorption sites could be occupied by Pb (II) ions and the available sites of adsorption would become fewer, hence the percentage removal of Pb (II) ions which depends upon the initial concentration could decrease (McSweeney JD, et al., 2006).

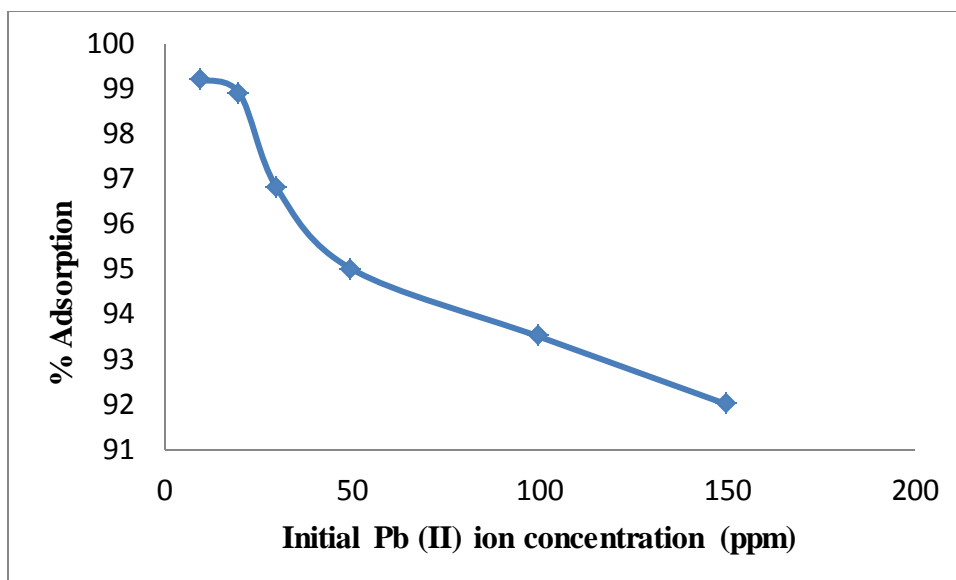


Figure 10. Effect of initial concentration of Pb (II) ions on the removal of Pb(II) ions, pH at 6, adsorbent dose = 2 g, agitation speed = 150 rpm and at optimized contact time).

#### 4.2.6. Kinetics of adsorption

By varying the contact time as; 1, 2, 4, 6, 8, and 10 hours through keeping all other parameters (pH, adsorbent dose, contact time, agitation speed and initial Pb (II) ions concentration) at optimized value helps for the determination of the effect of Pb (II) ions adsorption kinetics. On this study, the flow of the graph was almost similar to that of contact time except very insignificant modification were seen on the percent of adsorption, because it was done after optimization of agitation speed and initial metal ions concentration (Fig.11).

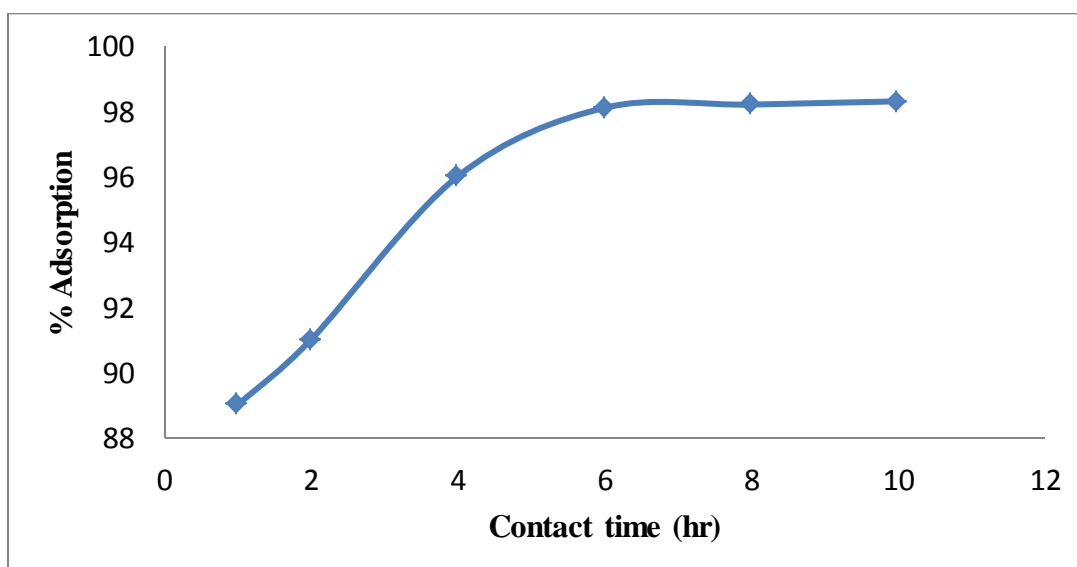
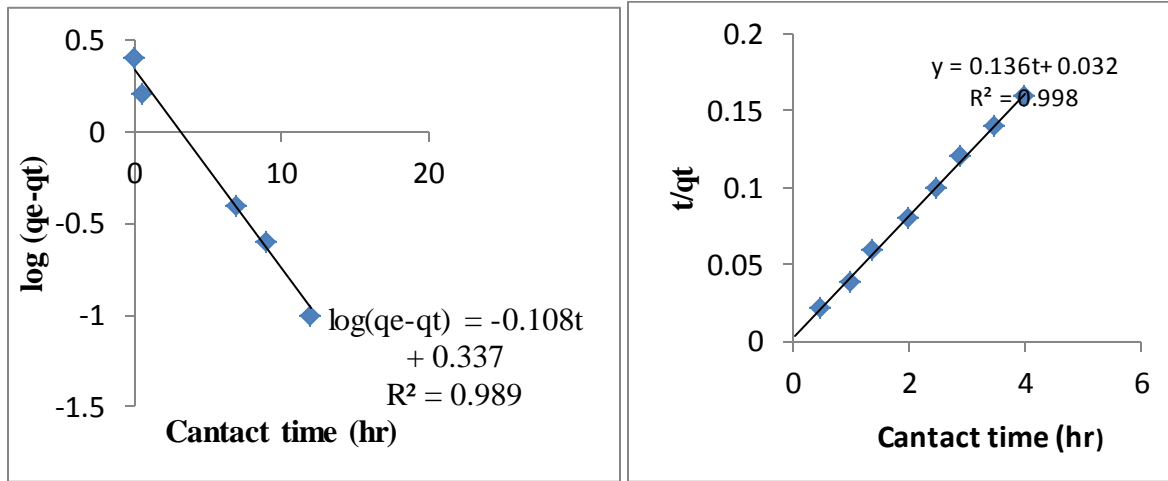


Figure 11. Kinetics of Adsorption on the removal of Pb(II) ions ( $C_0 = 10 \text{ mg/L}$  at  $\text{pH} = 6$ , adsorbent dose = 2 g, agitation speed = 150 rpm) in nanoparticle mixed with MC adsorbent system.

The kinetic curves obtained for the adsorption of Pb (II) ions from aqueous solutions onto the adsorbent (nanoparticle mixed with MC adsorbent) systems are shown (Fig.11).



a) b)

Figure 12. Plot of the pseudo-first (a) and pseudo-second (b) order model (At  $C_0 = 10 \text{ mg/L}$ ,  $\text{pH} = 6$ , adsorbent dose = 2 g and agitation speed = 150 rpm).

The first order rate constant  $k_1$  and equilibrium adsorption density  $q_e$  and the value of  $k_2$  and  $q_e$  were determined by using the slopes and intercepts of Pseudo-first order model [ $\log(q_e - q_t)$  vs  $t$ ] and Pseudo-second order model,  $t/q_t$  vs  $t$  (Figure 12 (a and b)) respectively. The kinetic parameters obtained from the models are given in table 4.

The experimental results of equilibrium capability for nanoparticle oxides mixed with MC adsorbent system was (7.36 mg/g), which shows that the first-order-kinetic model was not much correlated because it differs from the theoretical values. That mean it represents the initial stages where rapid adsorption occurs well but cannot be applied for the entire adsorption process. In contrast this, pseudo second-order reaction rate model provides high correlation value ( $R^2 = 0.998$  in nanoparticle mixed oxides with MC). Therefore, the study indicated that the pseudo-second order model better represents the metal ions adsorption kinetics, suggesting that more of the adsorption process might be chemisorptions.

The first order rate constant  $k_1$  and equilibrium adsorption density  $q_e$  were determined from the slopes and intercepts of Pseudo-first order model [ $\log(q_e - q_t)$  versus  $t$ ] (Figure 12a) and the value of  $q_e$  and  $k_2$  determined from the slopes and intercepts of Pseudo-second order model,  $t/q_t$  versus  $t$  (Figure 12b). The kinetic parameters obtained from the models are given in Table.2.

Table 2: Langmuir and Freundlich isotherm constants for Pb (II) ions adsorption by Fe-Al-MC sorbent

Adsorbent	Langmuir model				Freundlich model		
	$Q_o(\text{mg/g})$	$b$	$R_L$	$R^2$	$K_f$	$n$	$R^2$
Fe-Al-MC	40	0.56	0.056	0.997	1.0046	5.076	0.995

#### 4.2.7. Adsorption isotherm

The Freundlich isotherm model is an experimental relationship describing the adsorption of solutes from a liquid to a solid surface and assumes that different sites with several adsorption energies are involved (Limousin, G., et al., 2007). The Langmuir model supposes that there is no contact between the adsorbate molecules and the adsorption is restricted in a monolayer form (LimousinG, *et al.*, 2007). The linearized Langmuir and Freundlich plots are given in Figure.13 (a) and 12 (b) respectively. The slopes and intercepts of the linearized Freundlich and Langmuir plots were used to calculate the adsorption constants tabulated in Table 3. From Table 3, the higher correlation coefficients of Langmuir isotherm indicate that this model fits the adsorption data better than the Freundlich model.

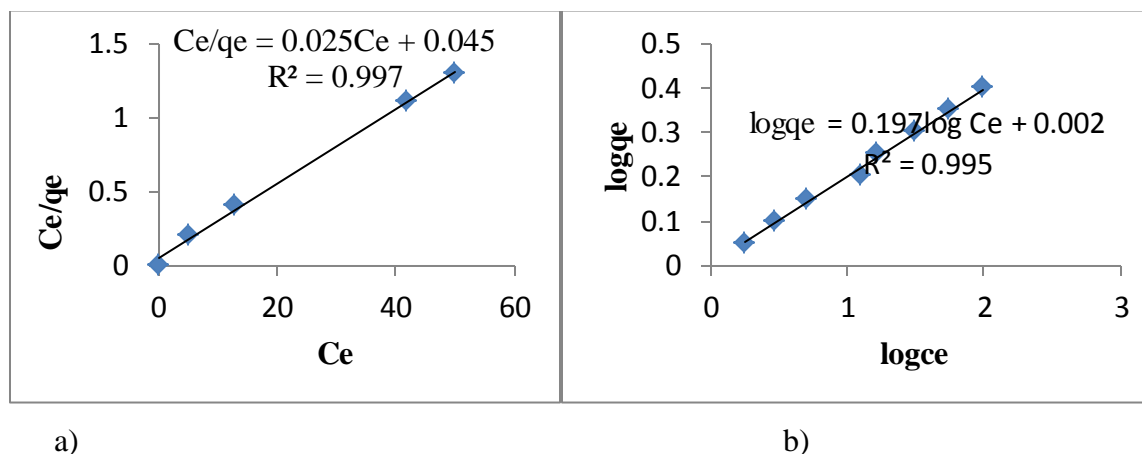


Figure 12. Langmuir (a) and Freundlich (b) adsorption isotherm of Pb<sup>2+</sup> ions by nanosized mixed oxide with MC sorbent at pH = 6.

The plot of  $C_e/q_e$  vs  $C_e$  yields a straight line with a slope, intercept,  $Q_0$  and  $b$  value of 0.025, 0.045, 40.00 and 0.56 respectively for NP-MC adsorbent (Figure .13 (a)).

A dimensionless equilibrium parameter (RL) value for all concentration is 0.056 which was in between 0 and 1 showing a favorable adsorption condition (Appendix Table.9). The plot of  $\log q_e$  vs  $\log C_e$ , yields a straight line with a slope 0.197 and an intercept 0.002 for NP-MC adsorbent. The value of  $1/n$  was found between 0 and 1 and equal to 0.197, for NP-MC adsorbent. The  $n$  value was (5.07) which is lying between 1 and 10, shows adsorption of  $Pb^{+2}$  ions onto adsorbent surface was easily carried out (Sairam *et al.*, 2009).

In this study, the values of correlation coefficient  $R^2$  for Fe-Al-MC adsorbent system were found to be = 0.997 and 0.995 for Langmuir and Freundlich model respectively, which confirms that both Langmuir and Freundlich models have the good representation of experimental data for the sorption isotherms of Pb (II) ions. Calculations for Pb (II) isotherms were listed in the appendix table 8. Linear equation used to calculate Langmuir, RL and Freundlich models are given in the literature equation (3, 4, 5 and 6), respectively.

Table 3: The values of parameters and correlation coefficients of kinetic models

	K	$q_e$ (mg/g)	$R^2$
Pseudo-first order	0.249	2.17	0.989
Pseudo-second order	0.578	7.36	0.998

#### 4.2.8. Thermodynamics of adsorption

The values of  $\Delta H^0$  and  $\Delta S^0$  were represented (Table 4.). The percentage of adsorption of metal ions increases with increasing temperature. The negative values of  $\Delta G^0$  and the positive values of  $\Delta H^0$  indicates the metal ion adsorption process was spontaneous and an endothermic respectively (Table.4).The decrease in  $\Delta G$  with the increase of temperature indicated more efficient adsorption at higher temperature (Unuabonah, E.I., et al., 2007). The positive value of solid/solution interface occurs in the internal structure of the metal ions and the NP-MC sorbent.

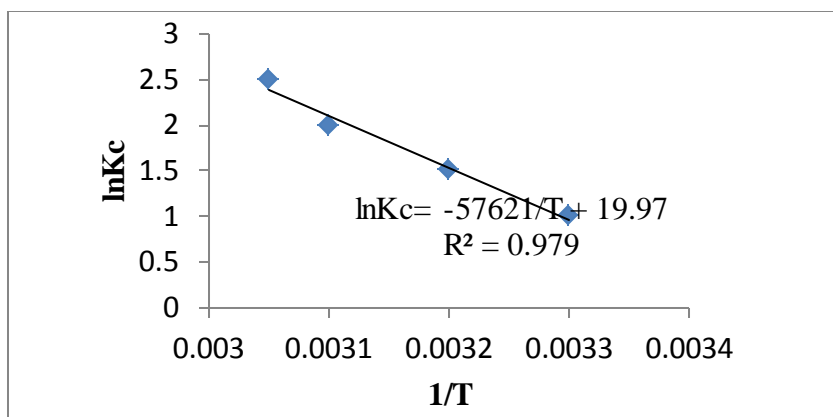


Figure 13. Plot of  $\ln K_c$  vs  $T^{-1}$  for Pb(II) ions adsorption in nanoparticle oxides mixed with MC adsorbent system, pH = 6, dose is 2 g, agitation speed = 150 rpm, time = 7 h,  $C_o = 10$  mg/L.

Table.4 Thermodynamic parameters for Pb(II) ions adsorption by Fe-Al-MC sorbent.

Adsorbent	T (K)	$\Delta G$ (KJ/mol)	$\Delta H$ (KJ/mol)	$\Delta S$ (J/mol k)
Fe-Al -MC	303	-2.402	+47.905	+166.03
	313	-4.062		
	333	-7.382		

#### 4.2.9. Desorption of lead

The Fe-Al-MC adsorbent was first saturated with  $Pb^{2+}$  ions of 10 mg/L. An adsorbent dosage of 2 g/L was added, and the mixture was shaken for 4 h. Then, the adsorbent was removed from the solution by HCl acid washing and again washed with deionized water five times. Desorption studies were conducted by shaking the Fe-Al-MC adsorbent adsorbed with Pb (II) ions with 0.1 M HCl for 4 h. The Fe-Al-MC adsorbent was separated from the solution by HCl washing and used for the subsequent adsorption-desorption cycle. According to the results of the desorption study (Figure 14), the amount of desorbed metal ions from the adsorbents i.e., nanoparticle mixed with MC was ranged from 10% at PH 2 to 65%, at  $P^H$  of (9). From this it is possible to conclude that, desorption process increases with increasing PH values (Salvador F., et al., 2015b).

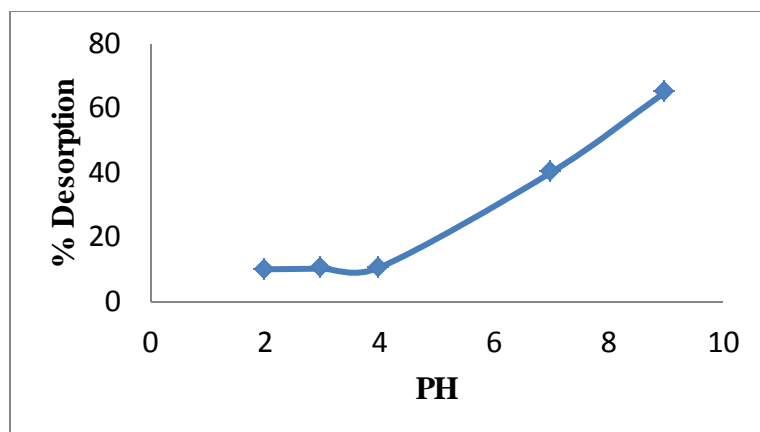


Figure 14. Effect of pH on desorption of Pb(II) ions in, nanoparticle oxide (NP) mixed with MC adsorbent, at varied pH.

#### 4.2.10. Comparison of the method with others

In comparison it is possible to observe the analytical performance of the Nano sorbent Fe-Al-MC with the other conventional sorbent system. The comparative data statistics about various sorbent systems is presented in table 5. The result shows that the adsorption capacity obtained by Fe-Al-MC adsorbent was comparable to those presented by other methods and has relatively high adsorption capacity (40 mg/g, greater than 98%) when compared to (Feng Y, et al., 2017; Feng, L, et al., 2012; Bhunia P, et al., 2018; Sun et al., 2018; Salihi, et al., 2017). Nevertheless, the proposed method is simpler than the others, for instance, there is no necessitate employing any complexing and/or chelating agent and the adsorbent is steady with a recycling period superior to chelating agent without major loss in its amounts and metal recovery property.

Table 5. Comparative data for different adsorbents adsorb different metals

Analyte	Adsorbents	Adsorption Capacity (mg g <sup>-1</sup> )	Reference
Cd(II)	Porous attapulgate/polymer beads	32.7mg/g	(Feng Y, et al., 2017)
As(v)	Fe <sub>3</sub> O <sub>4</sub>	16.56 mg/g	(Feng, L, et al., 2012)
Pb(II)	Chelating polyacrylonitrile beads	145 mg/g	(Bhunia P, et al., 2018)
Pb(II)	AC	23.4 mg/g	(Salihi, et al., 2017)
Pb(II)	Fe <sub>3</sub> O <sub>4</sub> /LDH-AM	266.6 mg/g	(Sun et al., 2018)
Pb(II)	Fe-Al-MC	40 mg/g	This work

## 5. CONCLUSION AND RCOMMENDATIONS

### 5.1. Conclusion

This work was aimed to evaluate the sorption efficiency of Fe-Al-MC sorbent developed from a chemical and local agricultural waste (Maize cob powder) for a toxic Pb (II) ions removal for wastewater remediation. The XRD result indicates that the Fe-Al-MC sorbent was amorphous and nanocrystalline. The SEM and EDX results showed that the surface morphologies and elemental compositions of the synthesized materials and heterogeneous nature of the sorbent. According to the batch study, the Pb (II) ions removal was found to be highly pH dependent whereas, maximum removal of the Pb (II) ions occurred at nearly neutral solution pH. Chemisorption process is the prevailing mechanism between the adsorbent and the adsorbate in pseudo-second order model which fitted best with the experimental data revealing the reusability and desorption repetition fulfilling the vital criteria for superior adsorbents. Both Freundlich and Langmuir isotherm models were used and from them the latter showing a better fit to the experimental data. Thermodynamic studies resulted in negative  $\Delta G$  value indicating the spontaneity of the sorption process. The Fe-Al-MC nanocomposite sorbent showed a sorption capacity of 40.00 mg g<sup>-1</sup> at pH 6. The sorption efficiency of the Fe-Al-MC sorbent was found to be 40 mg/g. Therefore, Fe-Al-MC adsorbent with large sorption capacity and efficiency is a promising and potential adsorbent for the removal of Pb (II) ions from the wastewater.

### 5.2. Recommendations

From the findings it is possible to conclude that the adsorbent shows that it is capable of removing Pb (II) ions from aqueous solution. Therefore, arising from the outcome of the study the following recommendations were made:

- Carry out the research on the removal capacity of these sorbent for other metals like Chromium, Cadmium, Mercury, etc.
- It is recommended to conduct a research on other efficient adsorbent system like electrochemically synthesized sorbent like carbon nanotube, for removal of heavy metals from aqueous solution.

- Optimize the removal efficiency of the nano-sized oxides mixed with MC adsorbent through continuous column experiment and any other chemical modification to increase the surface area of the adsorbent.

## 6. REFERENCES

- Agbenin, J.O. (2003): Extractable iron and aluminium effects on phosphate sorption in a Savanna Alfisol, *Soil Sci. Soc. Am. J.*, 67:589-595.
- Babel, S. and Kurniawan, T.A. (2003): Low-cost adsorbents for heavy metals uptake from contaminated water: a review. *J. Hazard. Mater.*, 97: 219-243.
- Badmus, M.A.O., Audu, T.O.K. and Anyata, B.U. (2007): Removal of Lead Ion from Industrial Wastewater by Activated Carbon Prepared from Periwinkle Shells (*Typanotonusfuscatus*). *Turkish Journal of Engineering and Environmental Sciences*, 31: 251-263.
- BuzuayehuAbebe, Abi M. Taddesse, TesfahunKebede, EndaleTeju, Isabel Diaz, (2017): Fe-Al-Mn ternary oxide nanosorbent: Synthesis, characterization and phosphate sorption property. *Journal of Environmental Chemical Engineering*, 5: 1330–1340.
- Chandan, B.P. (2008): Synthesis and Characterization of Alumina/Iron Oxide Mixed Nanocomposite. *Master of Science in chemistry national institute of technology*, Rourkela, 11, 4.
- Chen C., Wang X. (2006): Adsorption of Ni(II) from aqueous solution using oxidized multiwall carbon nanotubes. *Ind. Eng. Chem. Res.*, 45: 9144-9149.
- Chien, S.H. and W.R. Clayton (1980): Application of Elovich equation to the kinetics of phosphate release and sorption in soils, *Soil Sci. Soc. Am. J.*, 44: 265–268.
- Dong, X., H. Zou and W. Lin (2006): Effect of preparation condition of CuO-CeO<sub>2</sub>-ZrO<sub>2</sub> catalyst on CO removal from hydrogen rich gas, *international journal of hydrogen energy, Environmental Sanitation*, 6 (1): 1-13.
- Dong, C. Zhang, H. Pang, Z. Liu, Yu Zhang, Fulong(2013): Sulfonated modification of cotton linter and its application as adsorbent for high-efficiency removal of lead(II) in effluent. *Bioresour.Technol.*, 146:512–518.
- EPA Guidelines, (2007): Water and wastewater sampling, pp: 14-23.
- Feng, L., M. Cao, X. Ma, Y. Zhu and C. Hu (2012): Superparamagnetic high-surface-area Fe<sub>3</sub>O<sub>4</sub> nanoparticles as adsorbents for arsenic removal. *J. Hazard. Mater.* 217: 439-446.
- Freundlich, H. (1906): Uber die Adsorption in Losungen. *Zeitschriftfürphysik.Chemie*, 57: 385-470.
- Hadjmohammadi, M.R., M. Salary. and P. Biparva (2011): Removal of Cr (VI) from Aqueous Solution Using Pine Needles Powder as a Biosorbent. *Journal of Applied Sciences in Environmental Sanitation*, 6 (1): 1-13.

Hamdaoui, O. and M. Chiha (2007): Removal of Methylene Blue from Aqueous Solutions by Wheat Bran. *ActaChim.Slov.*, 54: 407–418.

Hardiljeet, K. Boparai, M. Joseph, D., O'Carroll, M. (2013): Cadmium ( $\text{Cd}^{2+}$ ) removal by nanozerovalent iron: surface analysis, effects of solution chemistry and surface complexation modeling. *Environ Sci. Pollut. Res.*, (20): 6210–6221.

(ICCEA, 2012): Preparation of Iron Oxide Nanoparticles Mixed with Calcinated Laterite for Arsenic Removal. September 8-9: Bangkok (Thailand).

John, C., Crittenden N. and Montgomery, W.H. (2005): Water treatment principles and design, John Wiley, Hoboken, N.J., 2<sup>nd</sup> edition, 685p.

Johnston, C.T. S. Wang, S.L. Hem, (2002): Measuring the surface area of aluminum hydroxide adjuvant. *J. Pharm. Sci.*, 91–1706 (7): 1702.

Kasuya, M. Teranishi, H. Aohima, K. Katoh, T. Horiguchi, N. Morikawa, Y. Nishijo, M. and Iwata, K. (1992): "Water pollution by cadmium and the onset of "itai-itai" disease," *Water Sci. Technol.*, vol. 25, pp. 149-156.

Koby M., Demirbas E., Senturk E., Ince M. (2005): Adsorption of heavy metal ions from aqueous solutions by activated carbon prepared from apricot stone. *Bioresour. Technol.*, 96: 1518-1521.

Kummel, R. and E. Worch (1990): Adsorption auswassrigenLosungen. Dt. Verl. FurGrundstoffindustrie, Leipzig, 1.auf. Edition, 272-285

Langmuir, I. (1918): the adsorption of gases on plane surfaces of glass, mica and platinum. *Journal of the American Chemical Society*, 40(9): 1361–1403.

Limousin, G., J. P. Gaudet, L. Charlet, S. Szenknect, V. Barthès, M. Krimissa (2007): Sorption isotherms: a review on physical bases, modeling and measurement. *Appl. Geochem.*, 22: 249–275.

Liu, P., Sehaqui, H., Tingaut, P., Wichser, A., Oksman, K., Mathew, A.P. (2014): Cellulose and chitin nanomaterials for capturing silver ions ( $\text{Ag}^+$ ) from water via surface adsorption., 21: 449–461.

Luciano Carlos, Fernando S. Garcia Einschlag, Monica C. Gonzalez and Daniel O. Martire (2013): Applications of Magnetite Nanoparticles for Heavy Metal Removal from Wastewater.<http://dx.doi.org/10.5772/54608>.

McSweeney JD, Rowell RM, Min SH (2006): Effect of citric acid modification of aspen wood on sorption of copper ion. *Journal of Natural Fibers.*, 3(1):43-58.

Mansoori, G.A., T. Rohani, A. Bastami, Z. Ahmadpour and Eshaghi (2008): Environmental

application of nanotechnology. *Annual Review of Nano Research*, 2, Chap. 2.

Oubagaranadin JUK, Murthy ZVP. (2009): Adsorption of divalent lead on a montmorilloniteillite type of clay. *Ind. Eng. Chem. Res.*, 48: 10627-10636.

O'Connell DW, Birkinshaw C, O'Dwyer TF (2008): Heavy metal adsorbents prepared from the modification of cellulose: a review. *BioresourTechnol*, 99(15): 6709–6724. doi:10.1016/j.biortech.2008.01.036.

O.R. Harvey, R.D. Rhue (2008): Kinetics and energetic of phosphate sorption in a multicomponent Al(III)-Fe(III) hydr (oxide) sorbent system, *J. Colloid Interface. Sci.*, 322: 384–393.

Pan B., Pan B., Zhang W., Lv L., Zhang Q. (2009): Development of polymeric and polymer-based hybrid adsorbents for pollutants removal from waters. *J. Chem. Eng.*, 151: 19-29.

Panneerselvam, P.N., N. Morad, K.A. Tan (2011): Magnetic nanoparticle (Fe<sub>3</sub>O<sub>4</sub>) impregnated onto tea waste for the removal of nickel(II) from aqueous solution. *Journals of Hazardous Materials*, 186: 160–168.

Rafika, S., Djilali, T., Benchreit, B., & Ali, B. (2009): Adsorption of heavy metals (Cd, Zn and Pb) from water using keratin powder prepared from algerien sheep hoofs. *European Journal of Scientific Research*, 35:416-425.

Raut, N. Charif, G. Amal Al-Saadi, Shinoona Al-Aisri, and Abrar Al-Ajmi (2012): “A Critical Review of Removal of Zinc from Wastewater,” *Proceedings of the World Congress on Engineering*, London, vol. I, July 4-6.

Rodic, D., M. Mitric, R. Tellgren, H. Rundlof, (2001): The cation distribution ...Y<sub>3</sub>Fe (5-x) Al<sub>x</sub>O<sub>12</sub>, *Journal of Magnetism and Magnetic Materials*, 232, 1-8.

Rodrigues, L.A. and M.C.P. Silva, (2009): An investigation of phosphate adsorption from aqueous solution onto hydrous niobium oxide prepared by co-precipitation method, *Colloids Surf.*, A 334, 191–196.

Sairam, C., N. Viswanathan and S. Meenakshi, (2009): Sorption behavior of fluoride on carboxylated cross linked chitosan beads. *J. Hazard. Mater.*, 11, 618-624.

Salvador F., Martin-Sanchez N, Sanchez-Hernandez R, Sanchez-Montero MJ and IzquierdoC. (2015b): Regeneration of carbonaceous adsorbents. Part II: Chemical, Microbiological and Vacuum Regeneration. *Micropor. Mesopor. Mat.*, 202: 277-296.

Satish P., D. Vajanta, R. Sameer and P. Naseema (2011): Kinetics of adsorption of crystal violet from aqueous solutions using different natural materials. *International Journal of Environmental science*, 1: 6.

Schumann, K. (1990): "The toxicological estimation of the heavy metal content (Cd, Hg, Pb) in food for infants and small children," *Z. Ernährungswiss.*, vol. 29, pp. 54-73.

SubrataMondal, (2017): Review Preparation, properties and applications of nanocellulosic materials. *Carbohydrate Polymers* 163: 301–316.

Sun S., Wang L., Wang A. (2006): Adsorption properties of crosslinkedcarboxymethyl-chitosan resin with Pb(II) as template ions. *J. Hazard. Mater.*, 136: 930-937.

Unuabonah, E.I., Adebowale, K. O., Olu-Owolabi, B. I. (2007): Kinetic and thermodynamic studies of the adsorption of lead (II) ions onto phosphate-modified kaolinite clay. *Journal of Hazardous Material*, 144: 386–395.

US EPA Method (2002): Sample Preparation Procedure for Spectrochemical Determination of Total Recoverable Elements, National Exposure Research Laboratory, Office of Water, US EPA, Cincinnati, OH.

USEPA., (2007): Nanotechnology white paper. ERA 100/B-07/001. Washington, DC 20460. Science Policy Council, U.S. *Environmental Protection Agency*, 120pp.

Wang J.L. And ChenC. (2006): "Biosorption of heavy metals by *Saccharomyces cerevisiae*: a review," *Biotechnol Adv.*, vol. 24, pp. 427-451.

Wang J.L. And Chen, C. (2009): "Biosorbents for heavy metals removal and their future a review," *Biotechnol, Adv.*, vol. 27, pp. 195-226.

Xu, Y., Axe, L. (2005): Synthesis and characterization of iron oxide-coated silica and its effect on metal adsorption. *J. Colloid. Interface. Sci.*, 282: 11–19.

Y. Feng, Y. Wang, Y. Wang, S. Liu, J. Jiang, C. Cao, J. Yao, (2017): Simple fabrication of easy handling millimeter-sized porous attapulgite/polymer beads for heavy metal removal. *J. Colloid. Interface Sci.*, 502: 52–58.

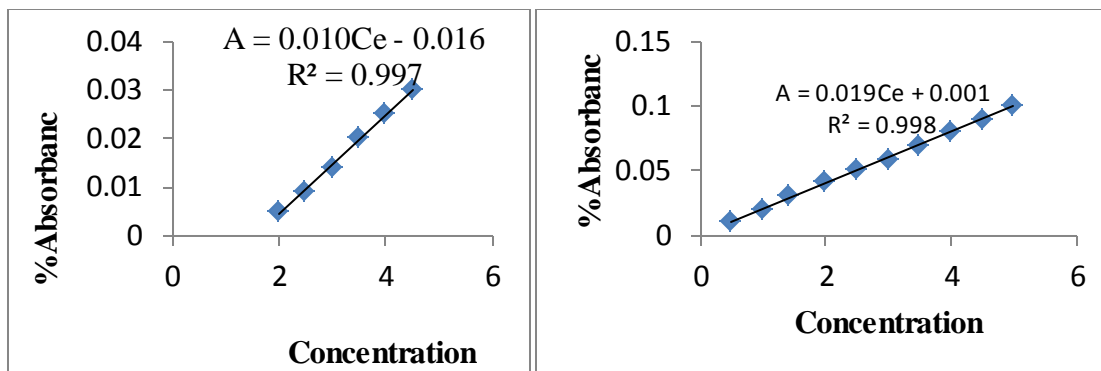
Yasuda, M. Miwa, A. and Kitagawa, M. (1995): "Morphometric Studies of renal lesions in "Itai-itai" disease: chronic cadmium nephropathy," *Nephron*, vol. 69, pp. 14-19.

Zhang, G. S., Qu, J. H., Liu, H. J., Liu, R. P., Wu, R. C. (2007): Fe-Mn binary oxide adsorbent for effective arsenic removal. *Water Research*, 41: 1921.

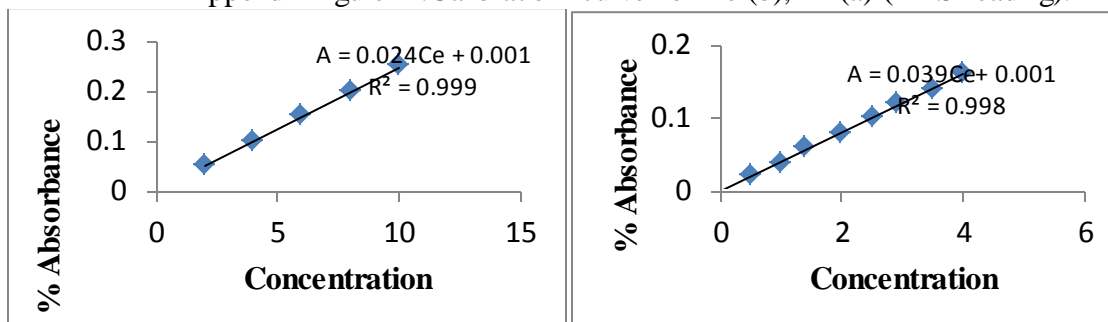
Zhao G., Li J., Ren X., Chen C., Wang X. (2011): Few-layered graphene oxide nanosheets as superior sorbents for heavy metal ion pollution management. *Environ SciTechnol* 45: 10454-10462.

Zhao X., Lv L., Pan B., Zhang W., Zhang *et al.* (2011): Polymer-supported nanocomposites for environmental application. A review: *J. Chem. Eng.*, 170: 381-394.

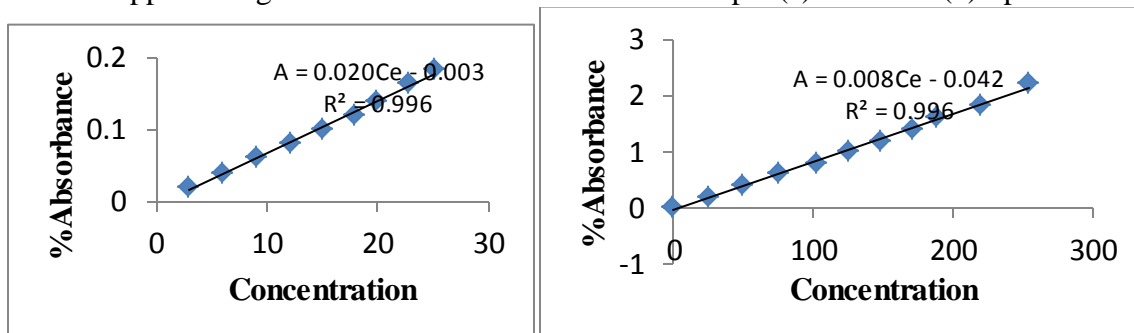
## **7. APPENDIX**



Appendix figure1 .Calibration curve for Fe (b), Al (a) (AAS reading).



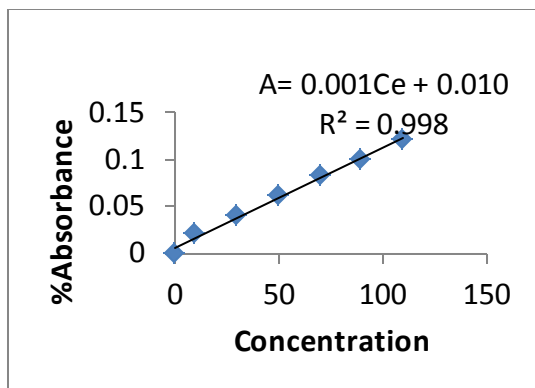
Appendix figure 2. Calibration curve of lead for pH (a) and dose (b) optimization.



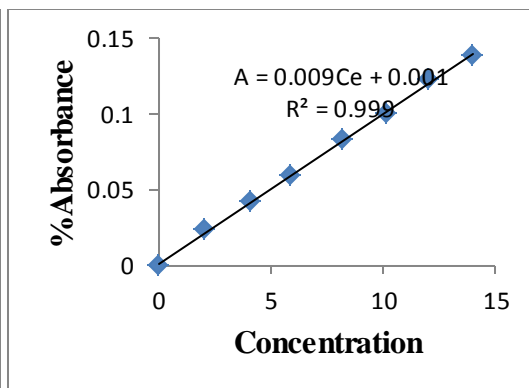
a)

b)

Appendix figure 3. Calibration curve of lead for contact time (a) and agitation speed (b) optimization.

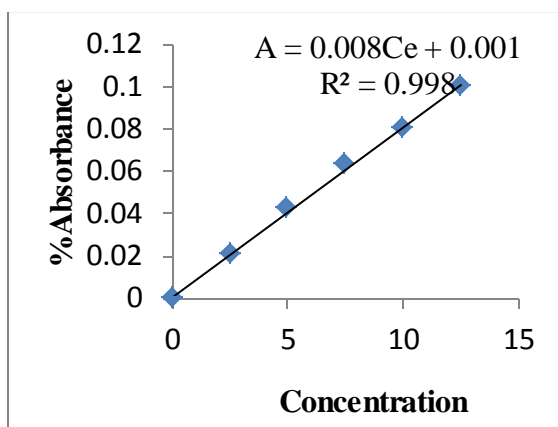


a)

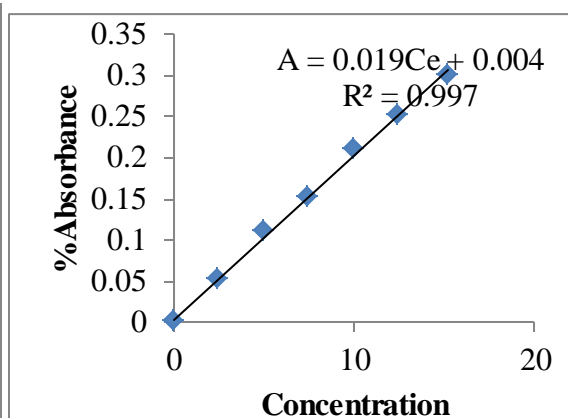


b)

Appendix figure 4. Calibration curve of lead (a) initial lead concentration optimization and kinetics adsorption study (b)

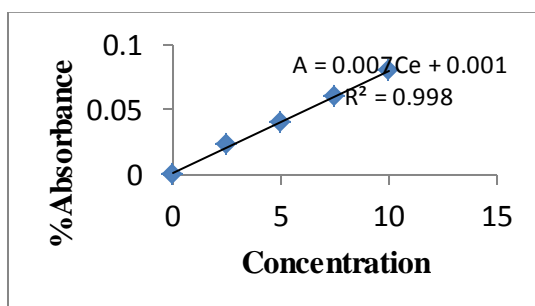


a)



b)

Appendix figure 5. Calibration curve of lead for selectivity (a) and thermodynamic study (b)



Appendix figure 6. Calibration curve of lead for desorption

Appendix Table 1. Designation of percentage composition of the as-synthesized powders calcined at 600°C and 400°C A and B respectively.

Temperature (°C)	Code of sample	Percentage (%) Composition		
		Fe	Al	MC
600	A	90	8	2
400	B	90	8	2

Appendix Table 2. Effect of pH on adsorption capacity of the nanoparticle mixed with maize cob adsorbents

p <sup>H</sup>	Ce (ppm)	%A	qe(mg/g)
2	3.60±0.009	88	6.60
4	3.60±0.009	92.5	6.94
6	3.60±0.009	98	7.35
8	3.60±0.009	98.2	7.37
9	3.60±0.009	98.3	7.38

Appendix Table 3. Effect of adsorbent dose on adsorption capacity of the nanoparticle mixed with maize cob adsorbents

Adsorbent dose (g)	Ce (ppm)	%A	qe(mg/g)
0.04	4.80±0.031	84	6.30
0.08	3.60± 0.272	88	6.60
0.16	0.90± 0.052	97	7.28
0.3	0.75± 0.255	97.5	7.32
0.5	0.60± 0.332	98	7.35
1	0.45± 0.04	98.5	7.39
<b>2</b>	0.39± 0.198	<b>98.7</b>	7.41
2.5	0.45± 0.200	98	7.35

Appendix Table 4. Effect of contact time on adsorption capacity of the nanoparticle mixed with maize cob adsorbents

Contact time (h)	Ce (ppm)	%A	qe(mg/g)
3	3.00±0.203	90	6.75
5	1.50± 0.002	95	7.12
<b>7</b>	0.60± 0.215	<b>98</b>	7.35
11	0.54± 0.098	98.2	7.36
21	0.51± 0.004	98.3	7.37
24	0.45± 0.004	98.5	7.39

Appendix Table 5. Effect of agitation speed on adsorption capacity of the nanoparticle mixed with maize cob adsorbents

Speed (rpm)	Ce (ppm)	% A	q <sub>e</sub> (mg/g)
100	0.87±0.340	97.10	7.28
<b>150</b>	0.30± 0.015	<b>99.00</b>	7.42
200	0.39± 2.002	98.7	7.41
250	0.51± 0.035	98.5	7.39
300	0.54± 0.004	98.2	7.36

Appendix Table 6. Effect of initial Pb (II) ion concentration on adsorption capacity of the nanoparticle mixed with maize cob adsorbents

Initial Pb (II) ion conc.(ppm)	Ce (ppm)	% A	q <sub>e</sub> (mg/g)
<b>10</b>	0.08±0.607	<b>99.2</b>	1.720
20	0.22± 1.050	98.9	4.390
30	0.96± 0.215	96.8	13.994
50	2.50± 0.098	95.0	23.340
100	6.51± 0.004	93.5	31.390
150	12.0± 0.004	92.0	34.823

Appendix Table 7. Effect of kinetic study on adsorption capacity of the nanoparticle mixed with maize cob adsorbents

Contact time (h)	Ce (ppm)	% A	t <sup>1/2</sup>	q <sub>t</sub> (mg/g)	log(q <sub>e</sub> -q <sub>t</sub> )	t/q <sub>t</sub>
1	3.32±0.372	89.00	1.15	6.67	-0.16	0.20
3	2.71± 0.512	91.00	1.76	6.82	-0.26	0.45
4	1.19±0.102	96.01	1.86	7.20	-0.79	0.48
6	0.56± 0.011	98.11	3.98	<b>7.36</b>		2.15
8	0.52± 0.504	98.21	3.99	7.37		2.16
10	0.50± 0.504	98.32	4.00	7.38		2.17

Appendix Table 8. Results for Pb (II) adsorption isotherm on adsorption capacity of the nanoparticle mixed with maize cob adsorbents

Conc.(ppm)	Ce (ppm)	Ce /q <sub>e</sub>	q <sub>e</sub> (mg/g)	logq <sub>e</sub>	logCe
10	0.08±0.607	0.046	1.720	0.2355	-1.097
20	0.22± 1.050	0.050	4.390	0.6425	-0.658
30	0.96± 0.215	0.0686	13.994	1.146	-0.018
50	2.50± 0.098	0.107	23.340	1.368	0.3979
100	6.51± 0.004	0.207	31.390	1.497	0.8129
150	12.0± 0.004	0.344	34.823	1.542	1.0792

Appendix Table 9. RL values for lead adsorption at different concentration.

Initial conc.(ppm)	RL
10	0.1515
20	0.082
30	0.056
50	0.034
100	0.018
150	0.012